Available online at www.sciencedirect.com
ScienceDirect
Mechanical Systems and Signal Processing 21 (2007) 3123–3145
Mechanical Systems and Signal Processing
www.elsevier.com/locate/jnlabr/ymssp

Linear system identification using proper orthogonal decomposition

Mohammad Khalil[a,*], Sondipon Adhikari[b], Abhijit Sarkar[a]

[a]*Department of Civil and Environmental Engineering, Carleton University, Mackenzie Building, Colonel By Drive, Ottawa, Ont., Canada K1S 5B6*

[b]*Department of Aerospace Engineering, University of Bristol, Queens Building, University Walk, Bristol BS8 1TR, UK*

Received 11 December 2006; received in revised form 15 March 2007; accepted 22 March 2007
Available online 4 April 2007

Abstract

A least-square-based method to identify the system matrices of linear dynamical systems is proposed. The primary focus is on the identification of a reduced-order model of the system operating in the mid-frequency range of vibration. Proper orthogonal decomposition (POD) is used for the model reduction. Such reduced-order model circumvents the limitations of traditional modal analysis which, although well-adapted in the low-frequency range, is prone to computational and conceptual difficulties in the mid-frequency range. The inverse problem involving the identification of the mass, damping and stiffness matrices is posed in the framework of a linear least-square estimation problem. To achieve this objective, Kronecker algebra is aptly exploited for a concise mathematical formulation to identify these matrix-valued variables. Tikhonov regularisation is used to satisfy the symmetry property of the system matrices. The application of the proposed methodology is demonstrated using an example of multiple degree-of-freedom discrete linear dynamical system. The robustness of the new methodology is investigated using a noise sensitivity study.

Keywords: System identification; Proper orthogonal decomposition; Tikhonov regularisation; Constrained least-squares estimation; Kronecker algebra; Mid-frequency range

1. Introduction

System identification plays a crucial role in the model-based prediction of dynamical systems. A finite representation of a continuous media described by a partial differential equation usually leads to a discrete dynamical system. In practical applications involving linear continuous operators, the discrete system is fully characterised by the so-called mass, stiffness and damping matrices. Once these matrices are estimated with reasonable confidence, such discrete model can predict the response of the underlying dynamical system to external disturbances. In the context of structural dynamics, the identification of these system matrices is achieved by traditional modal analysis techniques. In the low-frequency domain, only a few modes contribute to the total response of the system (see, for example, the books by Géradin and Rixen [1], Clough and Penzien

*Corresponding author. Tel.: +1 613 274 3427; fax: +1 613 526 1067.
E-mail address: mkhalil2@connect.carleton.ca (M. Khalil).

0888-3270/$ - see front matter © 2007 Elsevier Ltd. All rights reserved.
doi:10.1016/j.ymssp.2007.03.007

[2] and Humar [3]). Experimental modal analysis permits the extraction of such modal parameters through experimental measurements, as described by Maia and Silva [4] and Ewins [5]. The structure is set into motion by either a mechanical shaker, an impact hammer or ambient vibration (such as wind or traffic load in a bridge structure), with the corresponding response measured at one or more points. Recent innovation in the field of data-acquisition hardware allows us to acquire highly resolved spatio-temporal vibration data. For example, Iemma et al. [6] made use of the laser-vibrometer to conduct contact-free measurement of surface displacement of a structure.

For low-frequency vibration problems, the modal analysis has been widely used to identify the mass, stiffness and damping matrices from the measured response (see references [5,4,7–17] for example). The two main disadvantages of this approach are: (a) the accuracy of the identified modal parameters relies on the presence of distinct peaks in the measured frequency response functions (FRFs); (b) the identification of complex modes poses a serious challenge in the presence of non-proportional damping (refer to Srikantha-Phani and Woodhouse [18] and Adhikari [19]). The first problem is inherent to the conventional modal analysis. If the peaks in the measured FRFs are not distinct or are closely spaced, the modal parameter extraction procedure is difficult to apply [5]. As a consequence, the identified system matrices obtained using the extracted modal parameters become erroneous. It is therefore difficult to extend the modal identification procedure in the mid-frequency range where a large number of modes contribute to the total response. Modal analysis is also difficult to apply to periodic systems (such as the bladed disks in turbomachineries) inherently containing closely spaced modes demarcated by the so-called pass-bands and stop-bands [20]. The second problem arises for systems with high damping materials [21,22] such as panels with viscoelastic damping. In this paper, we investigate the ability to adopt a different approach to tackle the problem of system identification in the mid-frequency range. In order to be successful, such approach should address the following major challenges encountered in the mid-frequency range: (a) a high-resolution numerical model is needed to capture short wavelength system response leading to large-scale system matrices; (b) the small-amplitude system response may be significantly corrupted by noise. Any system identification tool must therefore be able to deal with, or at least bypass, significant computational costs associated with identifying the high-dimensional system matrices. Furthermore, the method must be robust in dealing with noise in the measured response data.

This paper explores the feasibility of identifying a proper orthogonal decomposition (POD)-based reduced-order model in mid-frequency structural dynamics. To reduce computational effort, such reduced-order model is exploited to identify the underlying dynamical system to be used as a predictive tool. POD is used to arrive at a low-dimensional representation of the system response. Kronecker algebra is exploited to achieve a concise formulation for the linear least-square identification problem in the matrix space. Tikhonov regularisation is applied to satisfy additional physical constraints in terms of the symmetric property of the system matrices. The robustness of the method is evaluated using a noise-sensitivity study. The paper is organised in the following manner. A brief background of POD is given in Section 2.1. The application of POD in reduced-order modelling is detailed in Section 2.2. In Section 3, the detailed formulation involving the system identification method is described. Section 4 describes the concept of Tikhonov regularisation and its application to system identification. A step-by-step algorithm of the proposed methodology is given in Section 5. Section 6 reports the results from a numerical example elucidating the feasibility and usefulness of the proposed method. The paper concludes in Section 7 where a summary and findings of the current investigation are detailed.

2. Reduced-order modelling

A fine spatial resolution of the finite element (FE) mesh is necessary to capture the local features of high- and mid-frequency vibration. The resulting FE model involves the solution of a large-scale linear system. Scalable algorithms involving domain decomposition methods [23–25] can tackle such large-scale systems through data parallelism by exploiting multi-processor computers. Nevertheless, reduced-order modelling offers a reasonable turnaround time in the forward simulation of systems having substantial model resolution. A reduced-order model is perhaps even more useful in tackling the inverse problem involving the identification of large-scale linear systems as many inversion algorithms perform better in identifying low-dimensional

models. We therefore aim to identify a reduced-order model to solve the problem of system identification in the mid-frequency range.

The primary issue in reduced-order modelling is the selection of a reduced-order basis to represent the response of a high-dimensional system. Such basis can be a natural choice as in the case of modal expansion or can be automated but explicitly identifiable as in Krylov method in iterative solvers [26,27]. The benefit derived from adopting a good set of basis functions depends on the problem at hand. Potential benefits include: (1) computational complexity reduction relative to the comprehensive model; (2) minimise turnaround time for repeated simulation; (3) extracting reusable basis for repeated computational tasks. A good basis is physically motivated and problem-dependent (e.g. POD basis), hierarchical (e.g. wavelet basis) or orthogonal (e.g. Fourier and POD basis). A physically motivated (therefore problem-dependent) basis splits the components of the result in a dominant part together with a subdominant part to enhance the accuracy further. A hierarchical basis separates different components by the scales of variations. Expansion in an orthogonal basis separates the components of the solution by decoupling the inner-product spaces. In the current investigation, we adopt a POD-based reduced-order model following [28–30].

We have chosen POD as a model reduction technique due to the following difficulties associated with modal analysis: (1) modal identification becomes problematical when the FRF is smooth or alternatively, when the natural frequencies are densely spaced in the frequency axis; (2) the form and magnitude of damping become significant in the mid-frequency band sometimes leading to complex modes due to non-proportional damping. Such complex modes do not necessarily form a *complete basis* in contrast to the case of POD basis. Furthermore, the effect of damping is included in the POD modes irrespective of its form (proportional or non-proportional) and magnitude.

2.1. Background of proper orthogonal decomposition

POD provides a basis for the spectral decomposition of a spatio-temporal signal and has been extensively used in numerous applications due to its various desirable properties. The most compelling property of POD is perhaps its mean-square optimality: it provides the most efficient way of capturing the dominant components of a high-dimensional signal with only a few dominant scales of fluctuations, namely proper orthogonal modes (POMs) [28–40]. POD has been used by Sarkar and Ghanem [28] and Sarkar and Paidoussis [29,30] for the model reduction of linear as well as non-linear dynamical systems [28–30]. In the context of system identification, POD has been applied by Kerschen and Golinval [31] and Feeny and Kappagantu [40] to measured displacements of a discrete undamped system with a known mass matrix leading to an estimation of the normal modes. The POD method has been used in the context of non-linear problems as a model-reduction tool by Azeez and Vakakis [32,33], Kerschen et al. [34–36] and Kunisch and Volkwein [37]. Lenaerts et al. [38,39] have used POD for the identification of a non-linear dynamical system whereby the non-linear stiffness parameter was identified with a reduced-order model. Other approaches for reduced-order identification of non-linear systems are detailed in [41]. The recent availability of data-acquisition hardware (such as the laser-vibrometer [6]) makes it possible to acquire highly resolved spatio-temporal vibration data rendering POD-based methods amenable to practical application.

The system of equations describing the forced vibration of a viscously damped linear discrete system with n degrees of freedom can be represented by

$$\mathbf{M}_n\ddot{\mathbf{u}}_n(t) + \mathbf{C}_n\dot{\mathbf{u}}_n(t) + \mathbf{K}_n\mathbf{u}_n(t) = \mathbf{f}_n(t). \tag{1}$$

Here $\mathbf{M}_n \in \mathbb{R}^{n\times n}$ is the mass matrix, $\mathbf{C}_n \in \mathbb{R}^{n\times n}$ is the damping matrix, $\mathbf{K}_n \in \mathbb{R}^{n\times n}$ is the stiffness matrix, $\mathbf{u}_n(t) \in \mathbb{R}^n$ is the displacement vector and $\mathbf{f}_n(t) \in \mathbb{R}^n$ is the forcing vector at time t. Our aim is to arrive at a POD-based reduced-order model of the above system of equations. Suppose that r snapshots of $\mathbf{u}$ are obtained at n locations (e.g., by using piezoelectric accelerometers) of a system response function. The response vector $\mathbf{u}(t)$ is normally stored in the discrete time format as

$$\mathbf{u}(t_i) = \begin{Bmatrix} u_1(t_i) \\ \vdots \\ u_n(t_i) \end{Bmatrix}, \tag{2}$$

where $t_i = i \times \delta t$ with δt being the uniform time step used in the data-acquisition card, $i = 1, \ldots, r$, and r is the total number of steps used in the measurement. One obtains the response correlation matrix $\mathbf{R}_{uu} \in \mathbb{R}^{n \times n}$ in the time domain to be used in the POD method as

$$\mathbf{R}_{uu} = \langle \mathbf{u}(t)\mathbf{u}^{\mathrm{T}}(t) \rangle, \tag{3}$$

where $\langle \cdot \rangle$ is the time averaging operator. The above matrix is symmetric and positive definite. In the case of the system being excited by band-limited incoherent stationary white noise vector of unit strength, the response correlation matrix can also be expressed in the continuous frequency domain [28,42] by

$$\mathbf{R}_{uu} = \int_B \Re\{\mathbf{H}^{\dagger}(\omega)\mathbf{H}(\omega)\}\, \mathrm{d}\omega. \tag{4}$$

Here $\mathbf{H}(\omega)$ denotes the system transfer matrix, $(\cdot)^{\dagger}$ is the complex conjugate transpose (Hermitian) operator and B is the frequency bandwidth of interest.

The spectral decomposition of $\mathbf{R}_{uu}$ is given by

$$\mathbf{R}_{uu} = \sum_{i=1}^{n} \lambda_i \boldsymbol{\varphi}_i \boldsymbol{\varphi}_i^{\mathrm{T}}, \tag{5}$$

where λ_i are the eigenvalues of $\mathbf{R}_{uu}$ and $\boldsymbol{\varphi}_i$ are the corresponding eigenvectors. The eigenvalues λ_i are arranged such that $\lambda_1 \geqslant \lambda_2 \geqslant \cdots \geqslant \lambda_n$. Due to the symmetry and positive definiteness of $\mathbf{R}_{uu}$, all eigenvalues are positive and the set of eigenvectors forms an orthonormal basis. Only the first few modes are the most important for the POD method since they capture most of the energy of the signal, i.e. $\mathbf{R}_{uu}$ can be approximated by

$$\mathbf{R}_{uu} \approx \sum_{i=1}^{m} \lambda_i \boldsymbol{\varphi}_i \boldsymbol{\varphi}_i^{\mathrm{T}}. \tag{6}$$

Here m is the number of dominant POD modes. Two widely used methods for determining the optimal dimension (m) of the reduced-order system are: (1) computing the percentage of energy extracted; (2) plotting the POD eigenvalues. Each λ_i represents the average energy contributed by each mode $\boldsymbol{\varphi}_i$ e.g., [43]. Thus by including more POD modes $\boldsymbol{\varphi}_i$, one increases the total percentage of energy captured by the reduced-order POD representation. The percentage of total energy extracted is computed by dividing the sum of the characteristic eigenvalues for the modes extracted by the sum of all the eigenvalues of the original correlation matrix as

$$\frac{\sum_{i=1}^{m} \lambda_i}{\sum_{i=1}^{n} \lambda_i} \geqslant \kappa, \tag{7}$$

assuming that POD is required to capture κ of the energy of the measured displacements. In general, m is much smaller than n. Furthermore, a narrower frequency band results in a smaller number of dominant modes being required for a good approximation.

The major tasks involved in POD are: (a) construction of the correlation matrix $\mathbf{R}_{uu}$ in Eq. (3) and (b) the solution of the eigenvalue problem in Eq. (5). These steps are straightforward compared to the effort involved in experimental modal analysis.

It is also important to note that the POD modes obtained are functions of the system response. Clearly, different inputs result in different outputs and, consequently, different POD modes are extracted. We are interested in determining the optimal set of POD modes which are equally valid for arbitrary excitations having their frequency contents confined within the prescribed frequency band. In order to excite the entire spectrum of natural frequencies in that frequency band, the system is forced to vibrate with an *incoherent* band-limited stationary vector white noise with unit strength [28,42], also known as "rain-on-the-roof" loading. The resulting response covariance matrix is thus given by Eq. (4) for this particular type of excitation.

2.2. System model reduction using POD

Let us consider the output vector $\mathbf{u}(t)$ of a multi-input multi-output system of order n. Having calculated the dominant subspace of POD, the output vector can be approximated by a linear representation involving the first m POD modes as

$$\mathbf{u}(t) \approx \sum_{i=1}^{m} a_i(t)\boldsymbol{\varphi}_i. \tag{8}$$

In matrix form, Eq. (8) becomes

$$\mathbf{u}(t) \approx [\boldsymbol{\varphi}_1, \ldots, \boldsymbol{\varphi}_m] \begin{Bmatrix} a_1(t) \\ \vdots \\ a_m(t) \end{Bmatrix}. \tag{9}$$

This can be rewritten as

$$\mathbf{u}(t) \approx \boldsymbol{\Sigma}\mathbf{a}(t), \tag{10}$$

where $\boldsymbol{\Sigma}$ is the transformation matrix containing the first m dominant POD eigenvectors:

$$\boldsymbol{\Sigma} = [\boldsymbol{\varphi}_1, \ldots, \boldsymbol{\varphi}_m] \in \mathbb{R}^{n\times m}, \tag{11}$$

and $\mathbf{a}(t)$ is the vector containing the respective coefficients. Eq. (10) indicates that system output is optimally approximated by applying a transformation $\boldsymbol{\Sigma}$ on the POD modal coefficient vector. The modal coefficients can be obtained by

$$\mathbf{a}(t) = \boldsymbol{\Sigma}^{\mathrm{T}}\mathbf{u}(t). \tag{12}$$

Each modal coefficient $a_i(t)$ is simply equal to the projection of the output vector $\mathbf{u}(t)$ onto the corresponding POD mode $\boldsymbol{\varphi}_i$.

Using the POD transformation matrix $\boldsymbol{\Sigma}$, the reduced-order representation of the system in Eq. (1) is

$$\mathbf{M}_m\ddot{\mathbf{u}}_m(t) + \mathbf{C}_m\dot{\mathbf{u}}_m(t) + \mathbf{K}_m\mathbf{u}_m(t) = \mathbf{f}_m(t), \tag{13}$$

where

$$\mathbf{M}_m = \boldsymbol{\Sigma}^{\mathrm{T}}\mathbf{M}_n\boldsymbol{\Sigma} \in \mathbb{R}^{m\times m}, \tag{14}$$

$$\mathbf{C}_m = \boldsymbol{\Sigma}^{\mathrm{T}}\mathbf{C}_n\boldsymbol{\Sigma} \in \mathbb{R}^{m\times m}, \tag{15}$$

$$\mathbf{K}_m = \boldsymbol{\Sigma}^{\mathrm{T}}\mathbf{K}_n\boldsymbol{\Sigma} \in \mathbb{R}^{m\times m}, \tag{16}$$

are the reduced-order mass, damping, and stiffness matrices, respectively. The reduced-order displacement vector (equivalent to the POD modal coefficients) and reduced-order forcing vector are given by

$$\mathbf{u}_m(t) = \boldsymbol{\Sigma}^{\mathrm{T}}\mathbf{u}_n(t) = \mathbf{a}(t), \tag{17}$$

$$\mathbf{f}_m(t) = \boldsymbol{\Sigma}^{\mathrm{T}}\mathbf{f}_n(t). \tag{18}$$

In the frequency domain, Eq. (13) is equivalent to

$$[-\omega^2\mathbf{M}_m + \mathrm{i}\omega\mathbf{C}_m + \mathbf{K}_m]\mathbf{U}_m(\omega) = \mathbf{F}_m(\omega), \tag{19}$$

where $\mathbf{U}_m(\omega) \in \mathbb{C}^m$ and $\mathbf{F}_m(\omega) \in \mathbb{C}^m$ are the Fourier transforms of $\mathbf{u}_m(t)$ and $\mathbf{f}_m(t)$, respectively.

Eq. (13) is the reduced-order model to be identified. Our task is to identify the reduced-order system matrices $\mathbf{M}_m$, $\mathbf{C}_m$ and $\mathbf{K}_m$. The value of $\mathbf{U}_m(\omega)$ is known from measurements and the value of $\mathbf{F}_m(\omega)$ is known as it is the input to the system. The proposed system identification technique can estimate the system matrices of both the comprehensive system in Eq. (1) as well as the reduced-order system in Eq. (13). In practice, however, the order of a complex system can be very high (in the order of millions) depending on the application at hand. In such cases the POD-based reduced-order model may reduce the identification problem

to estimating the reduced-order matrices of much smaller dimensions. From a computational perspective, the advantage of the reduced-order model identification problem relates to significant reduction of both the memory requirement and arithmetic complexity.

3. Reduced-order system identification

Consider the forced vibration of a viscously damped linear discrete system with m degrees of freedom described by Eq. (13) or (19). For a specific frequency ω_i, one can recast Eq. (19) as

$$[-\omega_i^2\mathbf{I}_m \quad \mathrm{i}\omega_i\mathbf{I}_m \quad \mathbf{I}_m]\begin{bmatrix}\mathbf{M}_m\\ \mathbf{C}_m\\ \mathbf{K}_m\end{bmatrix}\mathbf{U}_m(\omega_i)=\mathbf{F}_m(\omega_i). \tag{20}$$

Here $\mathbf{I}_m$ is the identity matrix of order m. Applying the vec operator (see Appendix A.2) on both sides of (20) and using the Kronecker algebraic identity $\mathrm{vec}(\mathbf{AYB})=(\mathbf{B}^{\mathrm{T}}\otimes\mathbf{A})\,\mathrm{vec}(\mathbf{Y})$ [44,45] we obtain

$$(\mathbf{U}_m(\omega_i)^{\mathrm{T}}\otimes[-\omega_i^2\mathbf{I}_m \quad \mathrm{i}\omega_i\mathbf{I}_m \quad \mathbf{I}_m])\mathrm{vec}\left(\begin{bmatrix}\mathbf{M}_m\\ \mathbf{C}_m\\ \mathbf{K}_m\end{bmatrix}\right)=\mathbf{F}_m(\omega_i). \tag{21}$$

Here $\otimes$ denotes the Kronecker matrix product (see Appendix A.1) and the unknowns are the elements of the mass, damping and stiffness matrices. Having measured the system response $\mathbf{U}_m(\omega)$ vector at s different frequencies and knowing the force $\mathbf{F}_m(\omega)$, one can rewrite Eq. (21) in the following augmented form:

$$\begin{bmatrix}\mathbf{U}_m(\omega_1)^{\mathrm{T}}\otimes[-\omega_1^2\mathbf{I}_m \quad \mathrm{i}\omega_1\mathbf{I}_m \quad \mathbf{I}_m]\\ \vdots\\ \mathbf{U}_m(\omega_s)^{\mathrm{T}}\otimes[-\omega_s^2\mathbf{I}_m \quad \mathrm{i}\omega_s\mathbf{I}_m \quad \mathbf{I}_m]\end{bmatrix}\mathrm{vec}\left(\begin{bmatrix}\mathbf{M}_m\\ \mathbf{C}_m\\ \mathbf{K}_m\end{bmatrix}\right)=\begin{Bmatrix}\mathbf{F}_m(\omega_1)\\ \vdots\\ \mathbf{F}_m(\omega_s)\end{Bmatrix}. \tag{22}$$

Eq. (22) is a system of equations and can thus be written as

$$\mathbf{Ax}=\mathbf{y}, \tag{23}$$

where

$$\mathbf{x}=\mathrm{vec}\left(\begin{bmatrix}\mathbf{M}_m\\ \mathbf{C}_m\\ \mathbf{K}_m\end{bmatrix}\right)\in\mathbb{R}^{3m^2}, \tag{24}$$

$$\mathbf{A}=\begin{bmatrix}\mathbf{U}_m(\omega_1)^{\mathrm{T}}\otimes[-\omega_1^2\mathbf{I}_m \quad \mathrm{i}\omega_1\mathbf{I}_m \quad \mathbf{I}_m]\\ \vdots\\ \mathbf{U}_m(\omega_s)^{\mathrm{T}}\otimes[-\omega_s^2\mathbf{I}_m \quad \mathrm{i}\omega_s\mathbf{I}_m \quad \mathbf{I}_m]\end{bmatrix}\in\mathbb{C}^{sm\times 3m^2} \tag{25}$$

and

$$\mathbf{y}=\begin{Bmatrix}\mathbf{F}_m(\omega_1)\\ \vdots\\ \mathbf{F}_m(\omega_s)\end{Bmatrix}\in\mathbb{C}^{sm}. \tag{26}$$

Eqs. (23)–(26) permit a convenient representation of the inverse problem involving identification of the matrix-valued unknown variables $\mathbf{M}_m$, $\mathbf{C}_m$ and $\mathbf{K}_m$ posed as the solution of a linear system of equations. The application of Kronecker identities allows such a concise and simple mathematical representation. The system of equations (22) is overdetermined in the case where $s>3m$. The vector $\mathbf{x}$ containing vectorised equivalent of

the mass, damping, and stiffness matrices can be solved in the least-square sense using the approximate inverse of the matrix $\mathbf{A}$ as follows:

$$\hat{\mathbf{x}} = [\mathbf{A}^{\mathrm{T}}\mathbf{A}]^{-1}\mathbf{A}^{\mathrm{T}}\mathbf{y}, \tag{27}$$

where $\hat{\mathbf{x}}$ is the least-square estimate of $\mathbf{x}$ and $[\mathbf{A}^{\mathrm{T}}\mathbf{A}]^{-1}\mathbf{A}^{\mathrm{T}}$ is the least-square inverse of matrix $\mathbf{A}$, also known as the Moore–Penrose inverse of a matrix [46,47].

The system matrix identification method proposed can identify the reduced order as well as the original model system matrices.

4. Tikhonov regularisation

4.1. Background

The estimated vector $\hat{\mathbf{x}}$ is a good solution to Eq. (23) if the matrix–vector product $\mathbf{A}\hat{\mathbf{x}}$ is close to $\mathbf{y}$. In the preceding section, the estimate of $\mathbf{x}$ is obtained in the least-squares sense. One quantity for measuring the accuracy of the estimated $\hat{\mathbf{x}}$ is the L_2-norm of the residual vector $\mathbf{A}\hat{\mathbf{x}} - \mathbf{y}$ given by

$$C(\hat{\mathbf{x}}) = \|\mathbf{A}\hat{\mathbf{x}} - \mathbf{y}\| = (\mathbf{A}\hat{\mathbf{x}} - \mathbf{y})^{\mathrm{T}}(\mathbf{A}\hat{\mathbf{x}} - \mathbf{y}). \tag{28}$$

Consider the case of the number of frequency points being relatively small due to insufficient measurements. In that case, the matrix $\mathbf{A}$ may have a rank less than $3m^2$ and there will exist one or more zero singular values of $\mathbf{A}$. The least-square solution vector $\hat{\mathbf{x}}$ will then have two components. One component lies in the subspace spanned by the singular vectors of $\mathbf{A}$ corresponding to the non-zero singular values. The other non-zero component exists in the subspace spanned by the singular vectors with zero singular values. Only the first component can reasonably be estimated from the data set $\mathbf{y}$.

Clearly there is a need to include additional information which permits the estimation of the component of $\mathbf{x}$ that lies in the null-space of $\mathbf{A}$. One approach to solving this problem is to introduce another norm $D(\hat{\mathbf{x}})$ that measures the error between $\hat{\mathbf{x}}$ and some default solution $\mathbf{x}^{\infty}$ where $\mathbf{x}^{\infty}$ may be some prior information about $\mathbf{x}$. $D(\hat{\mathbf{x}})$ has the form

$$D(\hat{\mathbf{x}}) = \|\hat{\mathbf{x}} - \mathbf{x}^{\infty}\|. \tag{29}$$

More generally, one strives to estimate the result of a linear operator $\mathbf{L}$ in the form of a matrix acting on the difference $(\hat{\mathbf{x}} - \mathbf{x}^{\infty})$ leading to

$$D(\hat{\mathbf{x}}) = \|\mathbf{L}(\hat{\mathbf{x}} - \mathbf{x}^{\infty})\| = (\hat{\mathbf{x}} - \mathbf{x}^{\infty})^{\mathrm{T}}\mathbf{L}^{\mathrm{T}}\mathbf{L}(\hat{\mathbf{x}} - \mathbf{x}^{\infty}). \tag{30}$$

A well-known regularisation technique is to form a weighted sum of $C(\mathbf{x})$ and $D(\mathbf{x})$ using a weighting factor λ^2. The estimate $\hat{\mathbf{x}}$ is the value of $\mathbf{x}$ that minimises this sum:

$$\hat{\mathbf{x}} = \arg\min\{C(\mathbf{x}) + \lambda^2 D(\mathbf{x})\}. \tag{31}$$

The solution to (31) can be obtained as

$$\hat{\mathbf{x}} = (\mathbf{A}^{\mathrm{T}}\mathbf{A} + \lambda^2\mathbf{L}^{\mathrm{T}}\mathbf{L})^{-1}(\mathbf{A}^{\mathrm{T}}\mathbf{y} + \lambda^2\mathbf{L}^{\mathrm{T}}\mathbf{L}\mathbf{x}^{\infty}). \tag{32}$$

The above formulation leads to a family of solutions parameterised by the weighing factor λ, popularly known as the *regularisation parameter* [48]. If the regularisation parameter is very large, the constraint involving the observed data $\mathbf{y}$ weakly influences the solution $\hat{\mathbf{x}}$. The estimate of $\mathbf{x}$ will be heavily dominated by the constraint $\mathbf{L}\mathbf{x} = \mathbf{L}\mathbf{x}^{\infty}$. On the other hand if λ is chosen to be small, the solution depends more heavily on the observed data. Of course, if λ is set to zero, the problem reduces to solving Eq. (23) being posed as an unconstrained optimisation problem. Thus, the value for the regularisation parameter is chosen based on how strongly one would like to enforce the constraint $\mathbf{L}\mathbf{x} = \mathbf{L}\mathbf{x}^{\infty}$. This regularisation method is generally known as Tikhonov regularisation [48].

4.2. Determination of the regularisation parameter

A main issue in applying Tikhonov regularisation is choosing a good value of λ that smoothes the solution without penalising the constraint on the available information. There are three methods to determine the optimal value for λ (see [49–52]):

(1) *Discrepancy principle*: Choose λ such that for a given value for ε, the residual norm satisfies

$$C(\widehat{\mathbf{x}}) = \varepsilon. \tag{33}$$

(2) *Generalised cross-validation principle*: Choose λ so as to minimise the function

$$G(\widehat{\mathbf{x}}) = \frac{\|\mathbf{A}\widehat{\mathbf{x}} - \mathbf{y}\|}{\mathrm{tr}(\mathbf{I} - \mathbf{A}(\mathbf{A}^{\mathrm{T}}\mathbf{A} + \lambda^2\mathbf{I})^{-1}\mathbf{A}^{\mathrm{T}})}. \tag{34}$$

where $\mathrm{tr}(\cdot)$ is the matrix trace operator. This method ensures that the regularisation parameter is invariant to an orthogonal transformation of the data.

(3) *L-curve criterion*: Choose λ that corresponds to the "corner" of the curve $\|\mathbf{A}\widehat{\mathbf{x}} - \mathbf{y}\|$ versus $\|\mathbf{L}(\widehat{\mathbf{x}} - \mathbf{x}^{\infty})\|$, plotted in log–log scale.

We have adopted the *L*-curve criterion in the current investigation.

4.3. Application to the system identification problem

In order to estimate the component of $\mathbf{x}$ that lies in the null-space of $\mathbf{A}$, one needs to include some prior knowledge concerning the system whenever any such information is available. For example, one can decide to arrive at a solution that enforces the estimated mass, stiffness and damping matrices to be symmetric, or as symmetric as possible. Such symmetry property in the discrete system matrices needs to be satisfied whenever the underlying continuous linear operator is self-adjoint. This problem can be posed as a constrained optimisation problem in the same theoretical framework detailed previously with certain modifications as discussed next.

In order to satisfy the symmetry, for instance, in the mass matrix $\mathbf{M}_m$, we need to have

$$\mathbf{M}_m = \mathbf{M}_m^{\mathrm{T}}. \tag{35}$$

With the aid of Kronecker algebra, the symmetry condition (35) in the mass matrix gives rise to the constraint equation (see Appendix B for the derivation):

$$\mathbf{L}_M\mathbf{x} = 0_{m^2}, \tag{36}$$

where

$$\mathbf{L}_M = (\mathbf{I}_m \otimes [\,\mathbf{I}_m \quad \mathbf{0}_{m\times m} \quad \mathbf{0}_{m\times m}\,]) - ([\,\mathbf{I}_m \quad \mathbf{0}_{m\times m} \quad \mathbf{0}_{m\times m}\,] \otimes \mathbf{I}_m)\mathbf{U}. \tag{37}$$

Here $\mathbf{U}$ denotes the vec-permutation matrix [53], $\mathbf{0}_{m^2}$ is the zero vector of order m^2, and the subscript in $\mathbf{L}_M$ indicates that the constraint is on the mass matrix.

The symmetry conditions on the damping matrix $\mathbf{C}_m$ and the stiffness matrix $\mathbf{K}_m$ similarly lead to

$$\mathbf{L}_C\mathbf{x} = 0_{m^2} \tag{38}$$

and

$$\mathbf{L}_K\mathbf{x} = 0_{m^2},$$

respectively, where

$$\mathbf{L}_C = (\mathbf{I}_m \otimes [\,\mathbf{0}_{m\times m} \quad \mathbf{I}_m \quad \mathbf{0}_{m\times m}\,]) - ([\,\mathbf{0}_{m\times m} \quad \mathbf{I}_m \quad \mathbf{0}_{m\times m}\,] \otimes \mathbf{I}_m)\mathbf{U}$$

and

$$\mathbf{L}_K = (\mathbf{I}_m \otimes [\,\mathbf{0}_{m\times m} \quad \mathbf{0}_{m\times m} \quad \mathbf{I}_m\,]) - ([\,\mathbf{0}_{m\times m} \quad \mathbf{0}_{m\times m} \quad \mathbf{I}_m\,] \otimes \mathbf{I}_m)\mathbf{U}. \tag{39}$$

Applying Tikhonov regularisation to estimate $\mathbf{x}$, we obtain the following solution:

$$\widehat{\mathbf{x}} = (\mathbf{A}^{\mathrm{T}}\mathbf{A} + \lambda_M^2\mathbf{L}_M^{\mathrm{T}}\mathbf{L}_M + \lambda_C^2\mathbf{L}_C^{\mathrm{T}}\mathbf{L}_C + \lambda_K^2\mathbf{L}_K^{\mathrm{T}}\mathbf{L}_K)^{-1}(\mathbf{A}^{\mathrm{T}}\mathbf{y}), \tag{40}$$

where $\mathbf{A}$ is defined in Eq. (25). The above solution depends on the values chosen for the regularisation parameters λ_M, λ_C and λ_K. If the regularisation parameters are very large, the constraint enforcing the symmetry condition is satisfied more accurately in $\mathbf{x}$ (the vector containing the elements of mass, damping and stiffness matrices).

5. Step-by-step summary of the proposed approach

The discussion so far leads to a simple algorithm for the system identification in linear structural dynamics. The method can be implemented by following these steps:

(1) From the band-limited system response, we form the response correlation matrix

$$\mathbf{R}_{uu} = \langle \mathbf{u}_n(t)\mathbf{u}_n^{\mathrm{T}}(t)\rangle. \tag{41}$$

(2) Decompose $\mathbf{R}_{uu}$ into its eigenvalues and eigenvectors

$$\mathbf{R}_{uu} = \sum_{i=1}^{n} \lambda_i \boldsymbol{\varphi}_i \boldsymbol{\varphi}_i^{\mathrm{T}} s \tag{42}$$

arranged such that $\lambda_1 \geqslant \lambda_2 \geqslant \cdots \geqslant \lambda_n$.

(3) Obtain the smallest value for the dimension of the reduced-order model (m) satisfying

$$\frac{\sum_{i=1}^{m}\lambda_i}{\sum_{i=1}^{n}\lambda_i} \geqslant \kappa, \tag{43}$$

assuming that POD is required to capture κth fraction of the energy of the signal.

(4) Obtain the transformation matrix containing the first m dominant POD eigenvectors:

$$\boldsymbol{\Sigma} = [\boldsymbol{\varphi}_1, \ldots, \boldsymbol{\varphi}_m] \in \mathbb{R}^{n\times m}. \tag{44}$$

(5) Obtain the POD reduced-order displacement vector and reduced-order forcing vector in the frequency domain

$$\mathbf{U}_m(\omega) = \boldsymbol{\Sigma}^{\mathrm{T}}\mathbf{U}_n(\omega) \tag{45}$$

and

$$\mathbf{F}_m(\omega) = \boldsymbol{\Sigma}^{\mathrm{T}}\mathbf{F}_n(\omega). \tag{46}$$

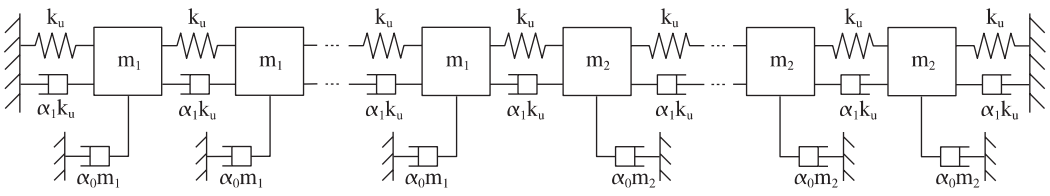

Fig. 1. Linear array of mass–spring oscillators.

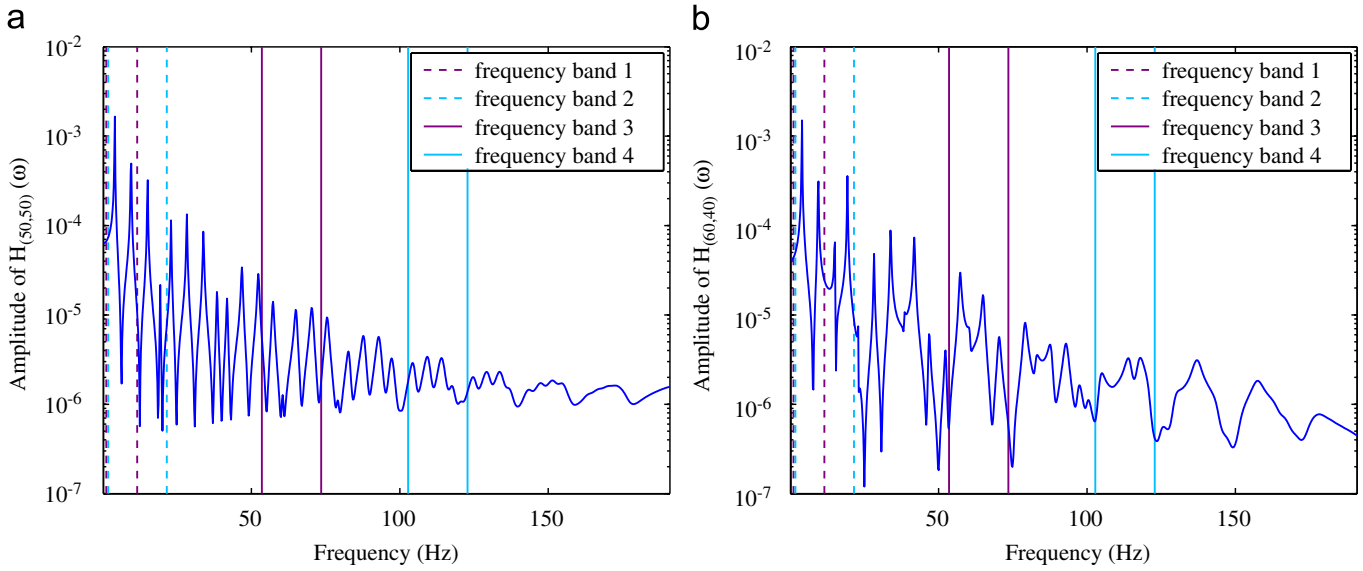

Fig. 2. Typical FRFs of original model along with the frequency bands of interest. (a) Driving-point-FRF and (b) cross-FRF.

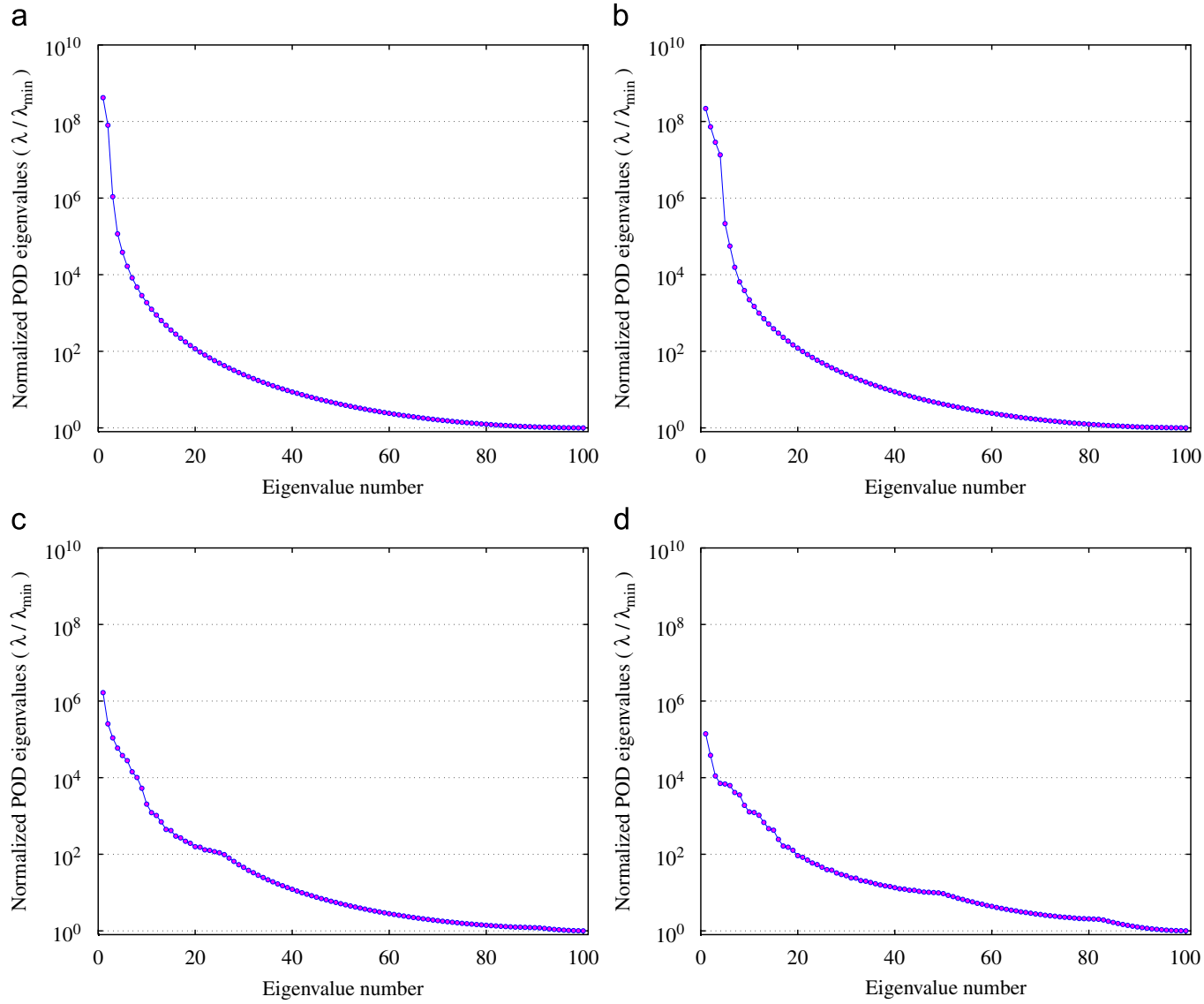

Fig. 3. Normalised POD eigenvalues (λ/λ_{max}) for (a) band 1, (b) band 2, (c) band 3, (d) band 4.

(6) Form

$$\mathbf{A} = \begin{bmatrix} \mathbf{U}_m(\omega_1)^{\mathrm{T}} \otimes [\,-\omega_1^2\mathbf{I}_m \quad \mathrm{i}\omega_1\mathbf{I}_m \quad \mathbf{I}_m\,] \\ \vdots \\ \mathbf{U}_m(\omega_s)^{\mathrm{T}} \otimes [\,-\omega_s^2\mathbf{I}_m \quad \mathrm{i}\omega_s\mathbf{I}_m \quad \mathbf{I}_m\,] \end{bmatrix} \quad \text{and} \quad \mathbf{y} = \begin{Bmatrix} \mathbf{F}_m(\omega_1) \\ \vdots \\ \mathbf{F}_m(\omega_s) \end{Bmatrix}. \tag{47}$$

(7) Form the symmetry-constraining matrices

$$\begin{aligned} \mathbf{L}_M &= (\mathbf{I}_m \otimes [\,\mathbf{I}_m \quad \mathbf{0}_{m\times m} \quad \mathbf{0}_{m\times m}\,]) - ([\,\mathbf{I}_m \quad \mathbf{0}_{m\times m} \quad \mathbf{0}_{m\times m}\,] \otimes \mathbf{I}_m)\mathbf{U}, \\ \mathbf{L}_C &= (\mathbf{I}_m \otimes [\,\mathbf{0}_{m\times m} \quad \mathbf{I}_m \quad \mathbf{0}_{m\times m}\,]) - ([\,\mathbf{0}_{m\times m} \quad \mathbf{I}_m \quad \mathbf{0}_{m\times m}\,] \otimes \mathbf{I}_m)\mathbf{U}, \\ \mathbf{L}_K &= (\mathbf{I}_m \otimes [\,\mathbf{0}_{m\times m} \quad \mathbf{0}_{m\times m} \quad \mathbf{I}_m\,]) - ([\,\mathbf{0}_{m\times m} \quad \mathbf{0}_{m\times m} \quad \mathbf{I}_m\,] \otimes \mathbf{I}_m)\mathbf{U}. \end{aligned} \tag{48}$$

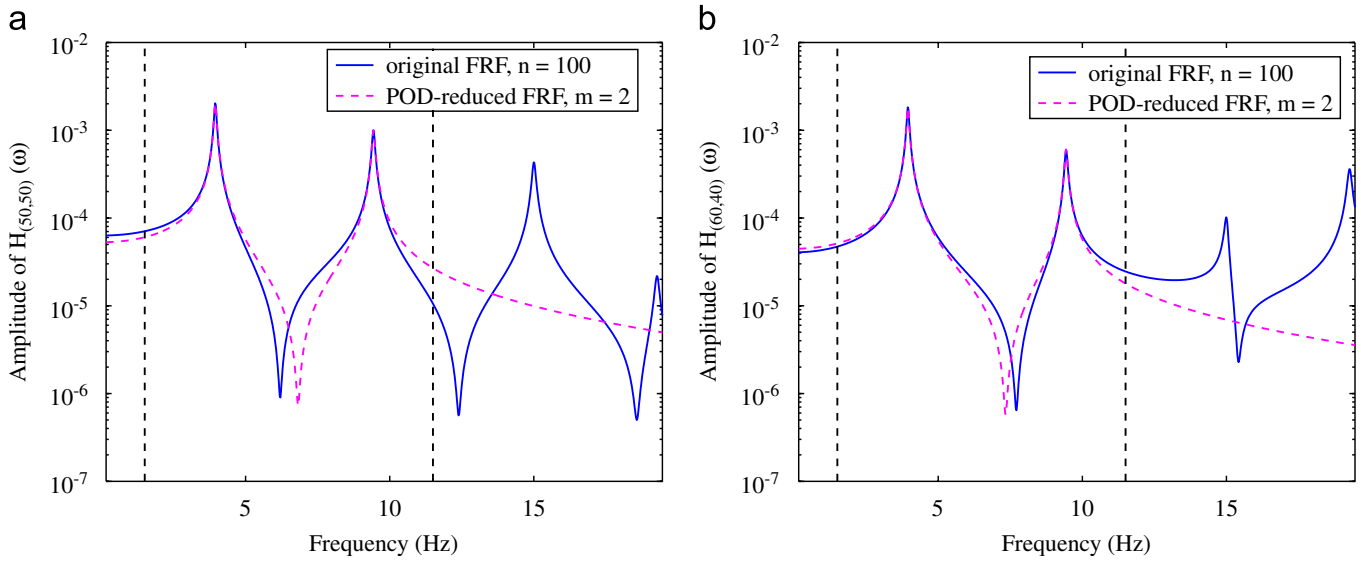

Fig. 4. Original and POD-reduced FRFs for frequency band 1. (a) Driving-point-FRF and (b) cross-FRF.

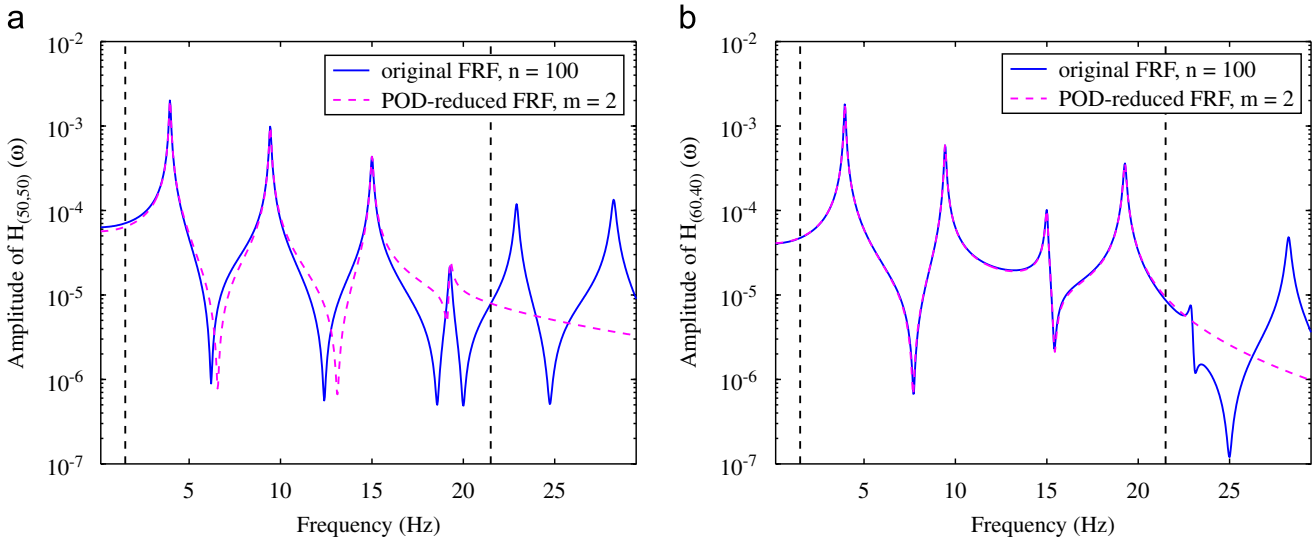

Fig. 5. Original and POD-reduced FRFs for frequency band 2. (a) Driving-point-FRF and (b) cross-FRF.

(8) Apply the inversion

$$\hat{\mathbf{x}} = (\mathbf{A}^{\mathrm{T}}\mathbf{A} + \lambda_M^2\mathbf{L}_M^{\mathrm{T}}\mathbf{L}_M + \lambda_C^2\mathbf{L}_C^{\mathrm{T}}\mathbf{L}_C + \lambda_K^2\mathbf{L}_K^{\mathrm{T}}\mathbf{L}_K)^{-1}(\mathbf{A}^{\mathrm{T}}\mathbf{y}) \tag{49}$$

choosing the values of λ_M, λ_C and λ_K as to satisfy the chosen criteria for determining the regularisation parameters.

(9) Obtain the estimated reduced-order mass, damping and stiffness matrices from $\hat{\mathbf{x}}$ satisfying

$$\hat{\mathbf{x}} \approx \mathrm{vec}\left(\begin{bmatrix}\mathbf{M}_m\\ \mathbf{C}_m\\ \mathbf{K}_m\end{bmatrix}\right). \tag{50}$$

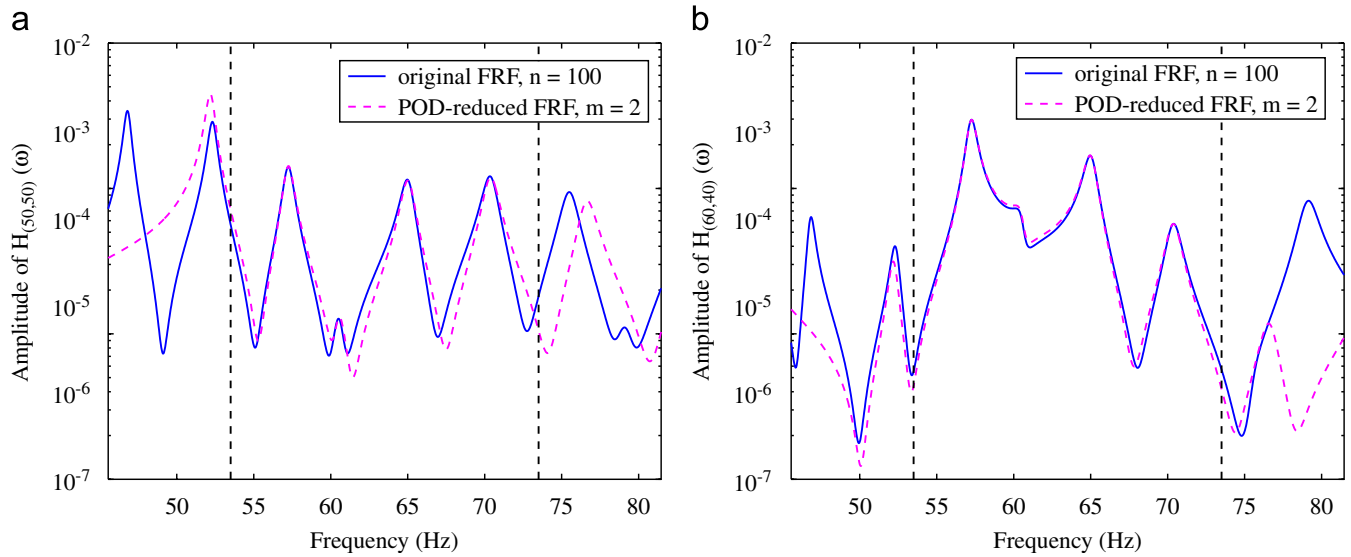

Fig. 6. Original and POD-reduced FRFs for frequency band 3. (a) Driving-point-FRF and (b) cross-FRF.

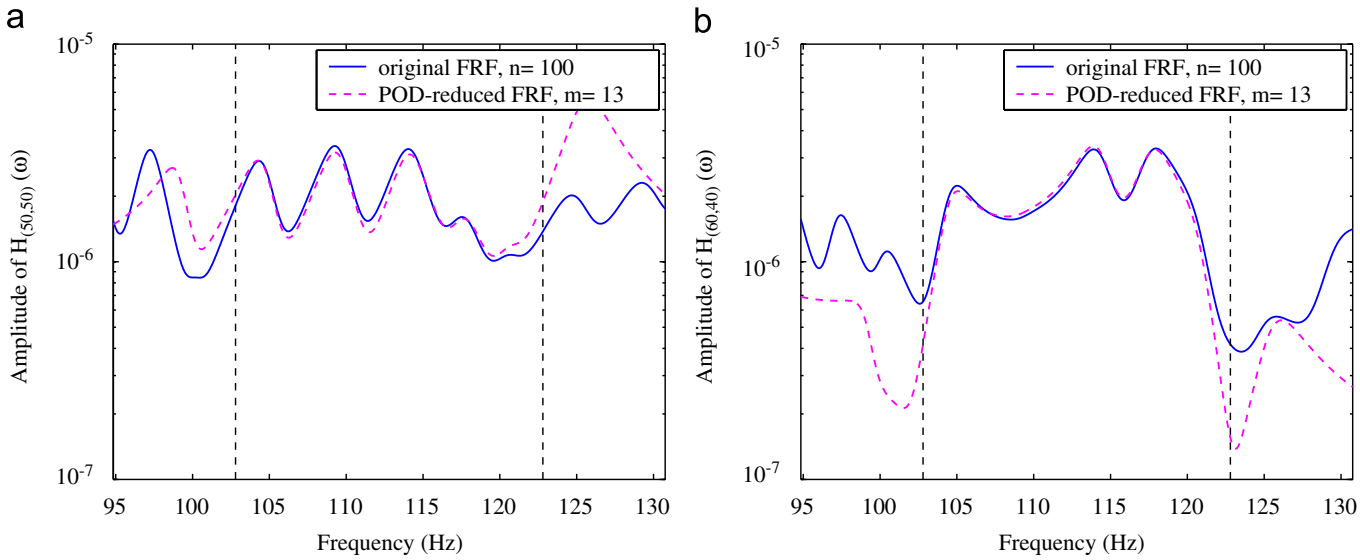

Fig. 7. Original and POD-reduced FRFs for frequency band 4. (a) Driving-point-FRF and (b) cross-FRF.

6. Numerical validation

In this section we consider a coupled linear array of mass–spring oscillators for a numerical illustration of the aforementioned mathematical formulation. Such discrete model normally arises from the FE discretisation of one-dimensional wave equation. At the initial stage these simple models are well-suited to investigate the usefulness and feasibility of the proposed methodology without the undue computational complexity involved in larger systems. In this example a lighter system is coupled with a heavier system. This simulates a scenario involving the dynamic interactions of two coupled subsystems with different modal densities.

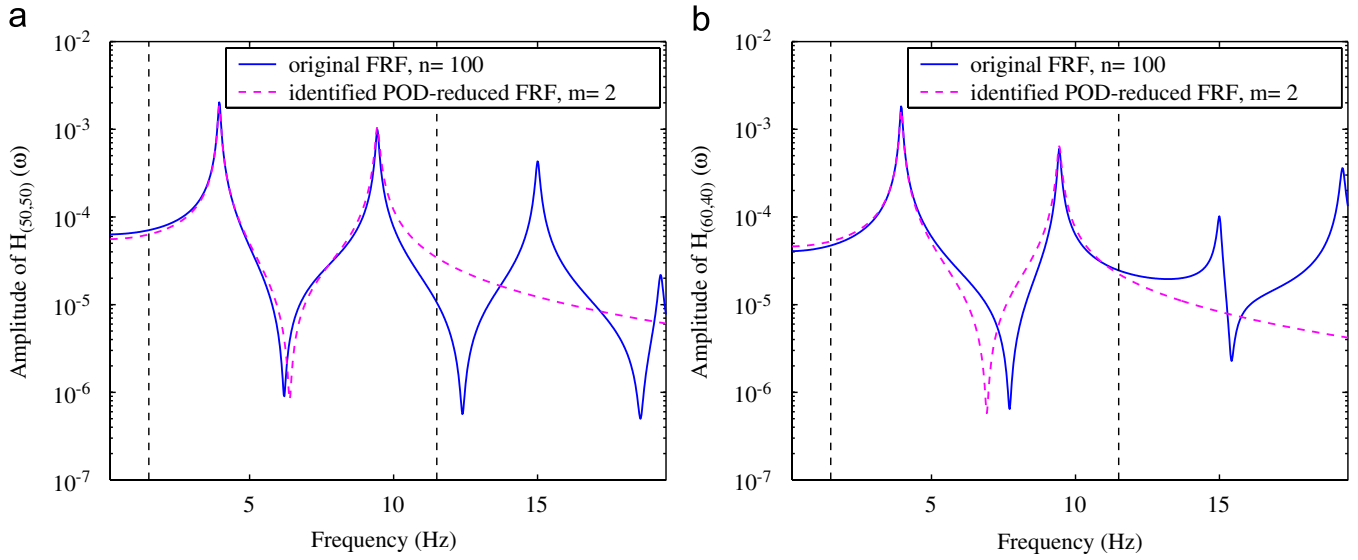

Fig. 8. Original and identified POD-reduced FRFs for frequency band 1. (a) Driving-point-FRF and (b) cross-FRF.

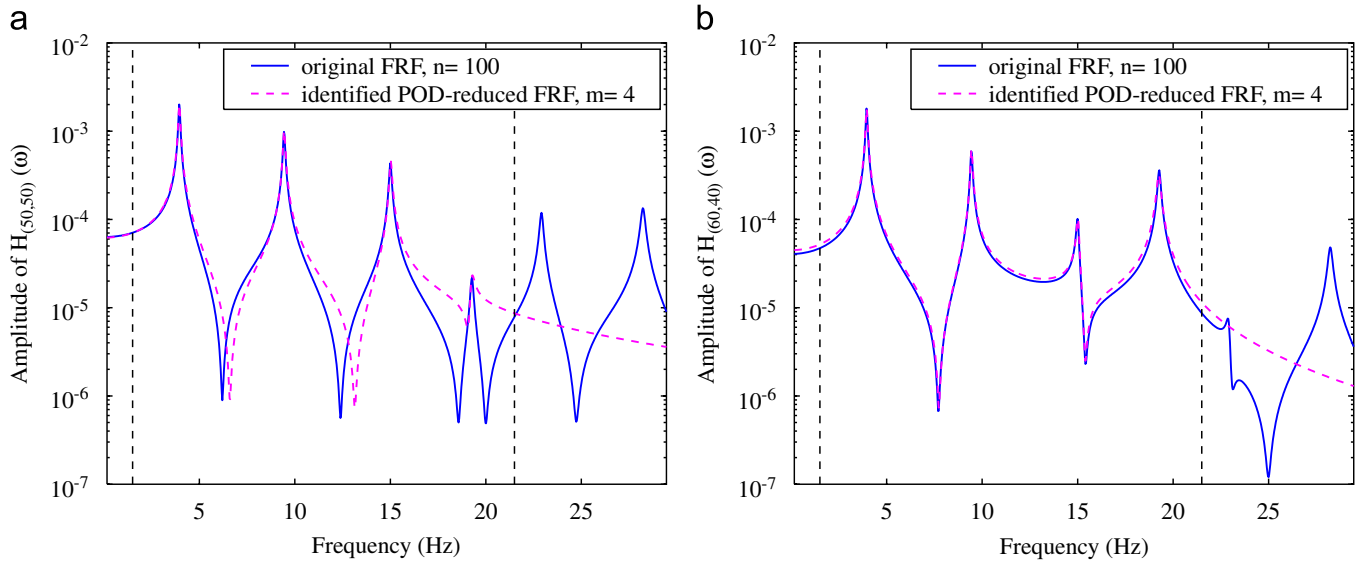

Fig. 9. Original and identified POD-reduced FRFs for frequency band 2. (a) Driving-point-FRF and (b) cross-FRF.

6.1. Original system model

The schematic diagram of the system is shown in Fig. 1. The mass matrix of the system has the form

$$\mathbf{M}_n = \begin{bmatrix} m_1\mathbf{I}_{n/2} & \mathbf{0}_{n/2\times n/2} \\ \mathbf{0}_{n/2\times n/2} & m_2\mathbf{I}_{n/2} \end{bmatrix}, \tag{51}$$

where n, m_1, and m_2 are chosen to be 100 DOFs, 0.1, and 1 kg, respectively. The stiffness matrix of the system is given by

$$\mathbf{K}_n = k_u \begin{bmatrix} 2 & -1 & & \\ -1 & \ddots & \ddots & \\ & \ddots & \ddots & -1 \\ & & -1 & 2 \end{bmatrix}, \tag{52}$$

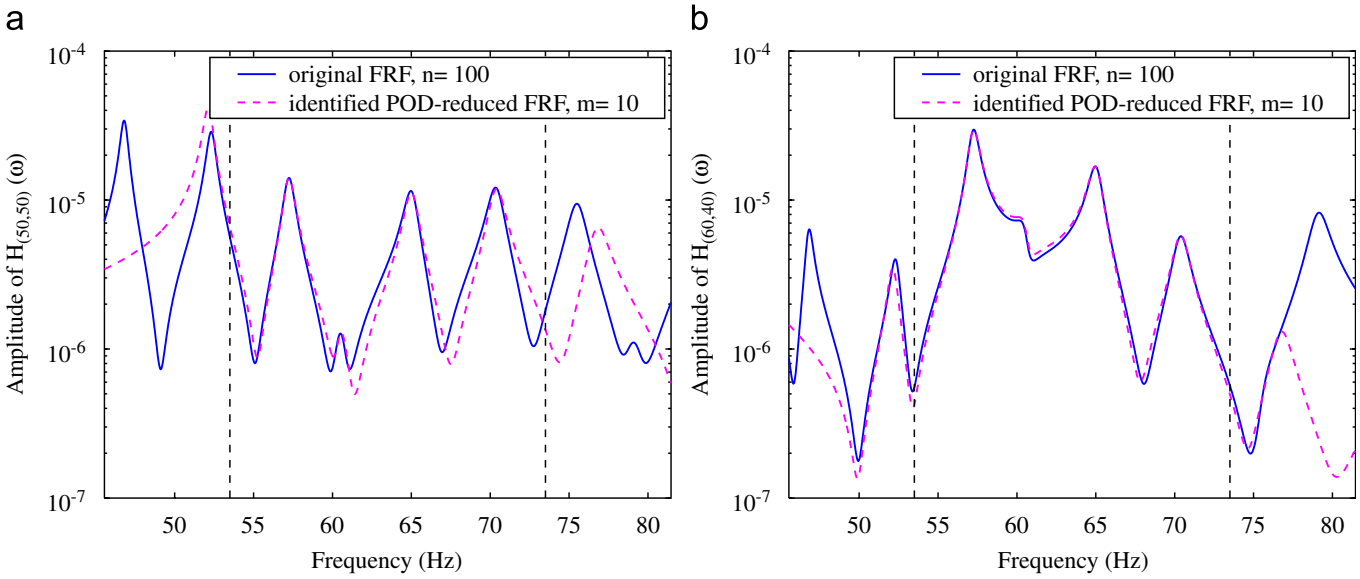

Fig. 10. Original and identified POD-reduced FRFs for frequency band 3. (a) Driving-point-FRF and (b) cross-FRF.

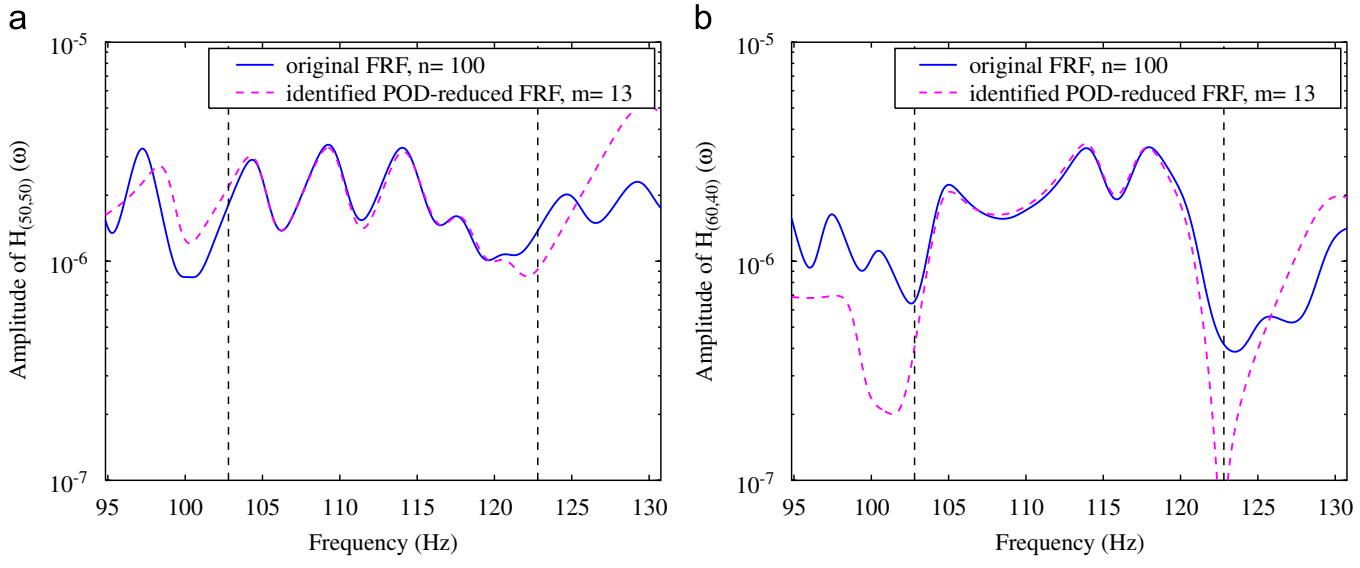

Fig. 11. Original and identified POD-reduced FRFs for frequency band 4. (a) Driving-point-FRF and (b) cross-FRF.

with $k_u = 4 \times 10^5$ N/m. Energy dissipation in the system is modeled by Rayleigh damping given by $\mathbf{C}_n = \alpha_0 \mathbf{M}_n + \alpha_1 \mathbf{K}_n$, where $\alpha_0 = 0.5$ and $\alpha_1 = 3 \times 10^{-5}$. Four frequency bands are considered for the construction of the POD-based reduced-order model:

(1) *Band* 1: Low-frequency band (1.5–11.5) Hz.
(2) *Band* 2: Low-frequency band (1.5–21.5) Hz.
(3) *Band* 3: Intermediate-frequency band (53.5–73.5) Hz.
(4) *Band* 4: Mid-frequency band (102.8–122.8) Hz.

These frequency bands are shown in the cross- and driving-point-FRFs of the system in Fig. 2. Next we construct the POD-based reduced model which adapts with the frequency band of interest.

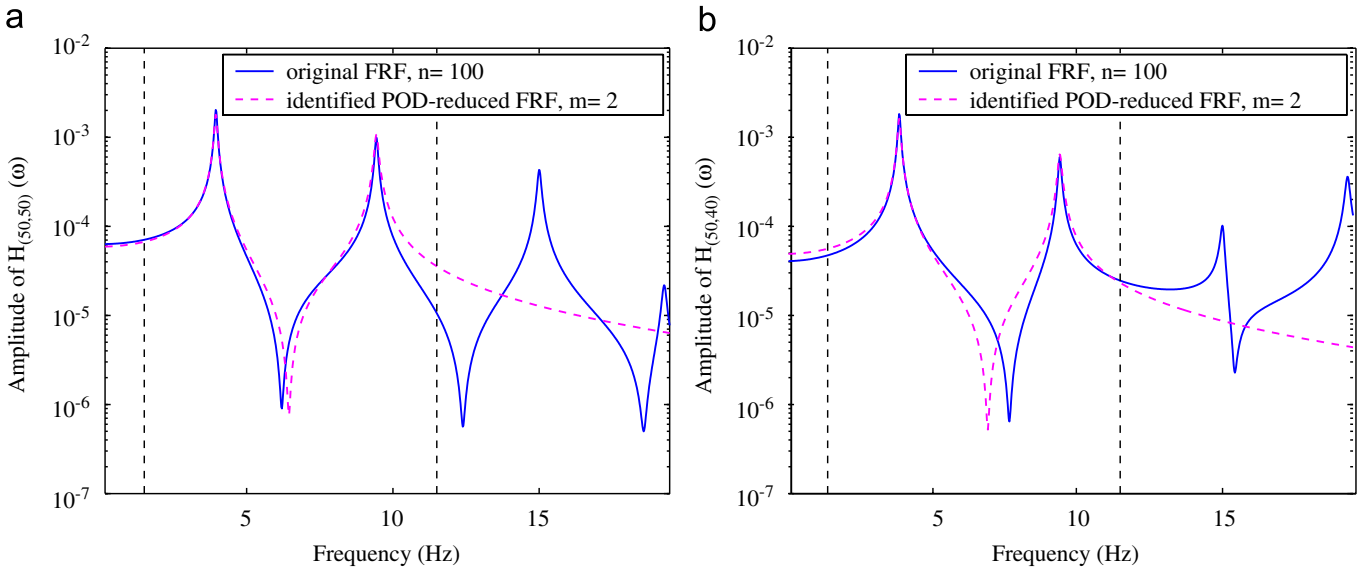

Fig. 12. Original and identified POD-reduced FRFs under an SNR of 20 dB for frequency band 1. (a) Driving-point-FRF and (b) cross-FRF.

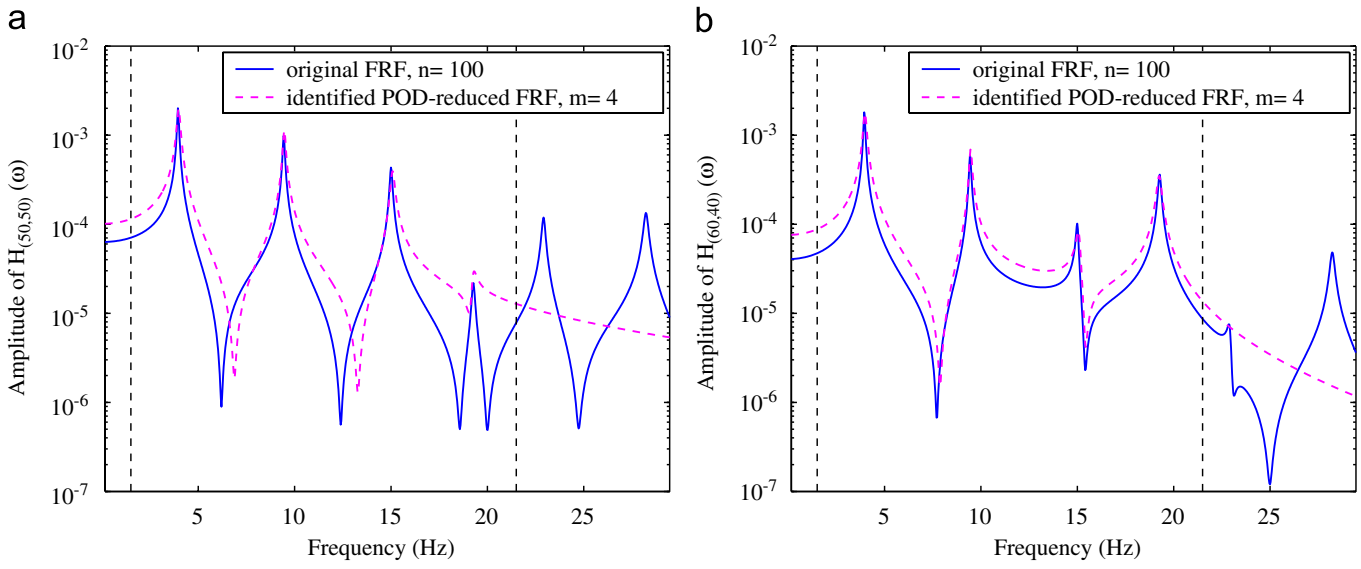

Fig. 13. Original and identified POD-reduced FRFs under an SNR of 20 dB for frequency band 2. (a) Driving-point-FRF and (b) cross-FRF.

6.2. Reduced-order model: forward simulation

Under a band-limited independent white noise input with unit variance, the system response is used to construct the correlation matrix. The POD eigenvectors are now extracted from the correlation matrix for each of the four frequency bands. Normalised eigenvalues of the correlation matrix, that is $\lambda/\lambda_{\max}$, are shown in Fig. 3. Examining all four plots of Fig. 3, only the first few eigenvalues are significantly large as expected. This justifies the approximation in Eq. (6).

Typical cross-FRFs and driving-point-FRFs of the POD-based reduced-order model are compared with the original FRFs in Figs. 4–7. Examining these figures, it is clear that the FRFs from the POD-based reduced-order models match reasonably well with the original FRF in the frequency bands of interests. Comparing Fig. 4 with Fig. 5, it can be seen that extending the frequency bandwidth increases the dimensions of the reduced-order models. Furthermore, note from Figs. 5–7 that the greater number of POMs are required for

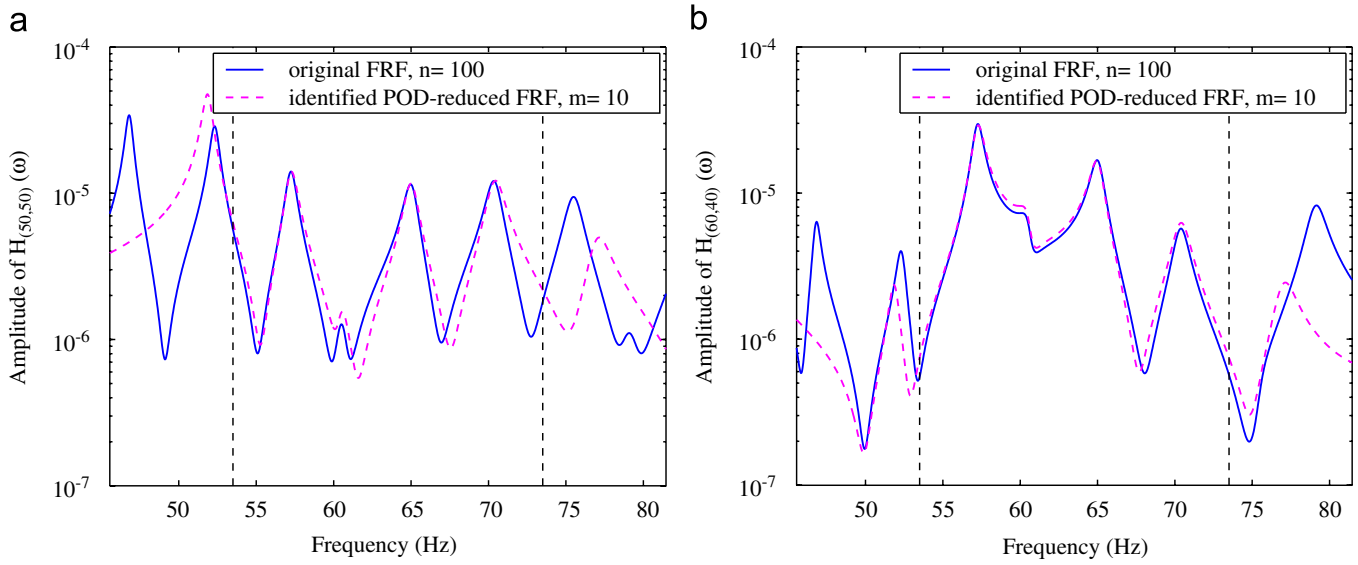

Fig. 14. Original and identified POD-reduced FRFs under an SNR of 20 dB for frequency band 3. (a) Driving-point-FRF and (b) cross-FRF.

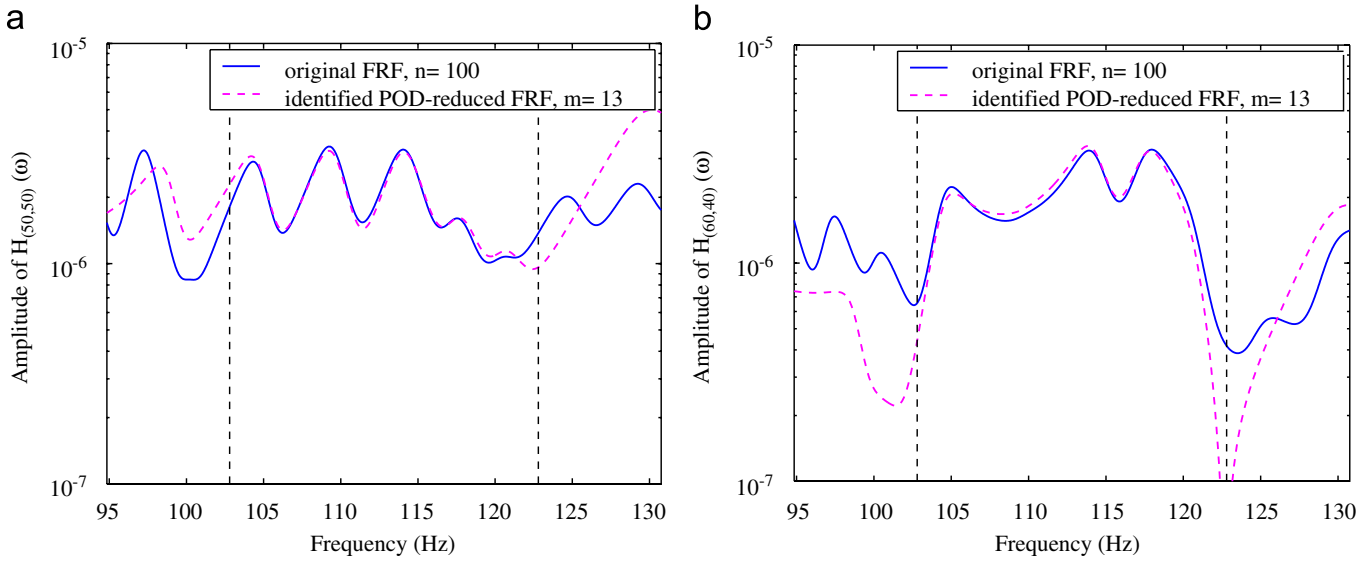

Fig. 15. Original and identified POD-reduced FRFs under an SNR of 20 dB for frequency band 4. (a) Driving-point-FRF and (b) cross-FRF.

the reduced models at higher frequencies. The FRFs of the reduced models do not match well the FRFs of the original system outside the frequency band of interest. This is expected as the POD-based reduced models are only adapted to the frequency band of the measured response used for the extraction of POMs. There are a number of factors that influence the accuracy of the reconstructed FRFs, for example (a) number of POD modes to retain, (b) level of damping and (c) the size and position of frequency window for the construction of POD.

6.2.1. *Reduced-order model identification: noiseless case*

Here we consider the inverse problem to identify the reduced system matrices using the proposed method in the ideal case when the measured response is noise-free. Subsequently, we consider the case of a noise-contaminated output. Using the measured response, the dimension of the reduced model can be determined *a*

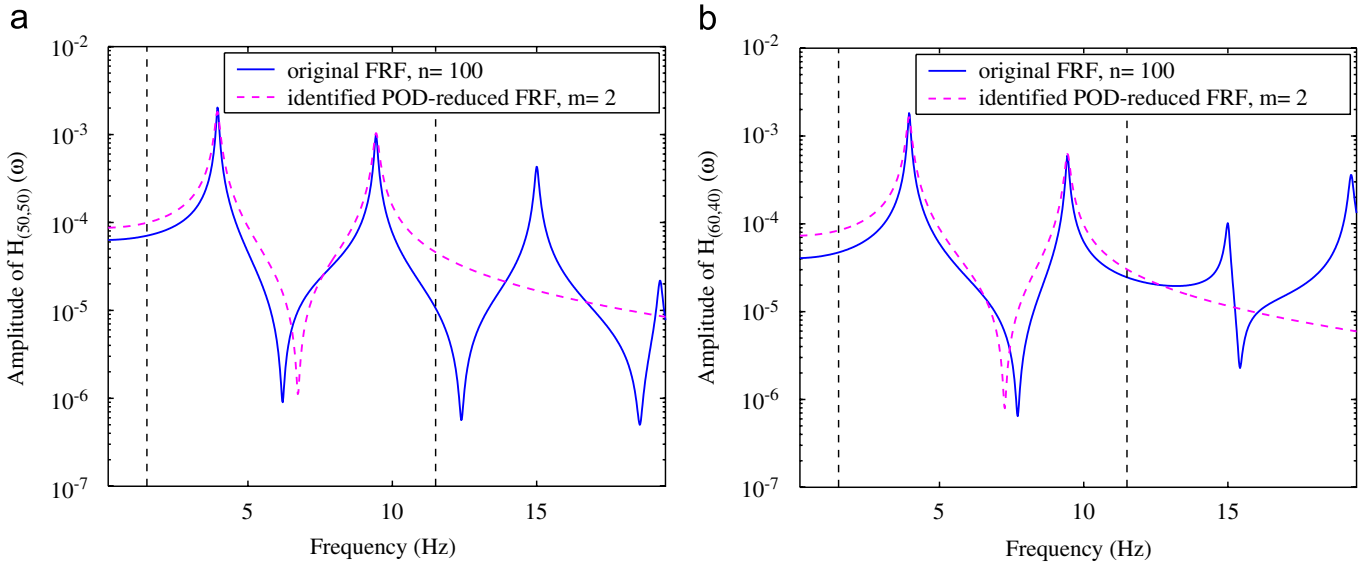

Fig. 16. Original and identified POD-reduced FRFs under an SNR of 10 dB for frequency band 1. (a) Driving-point-FRF and (b) cross-FRF.

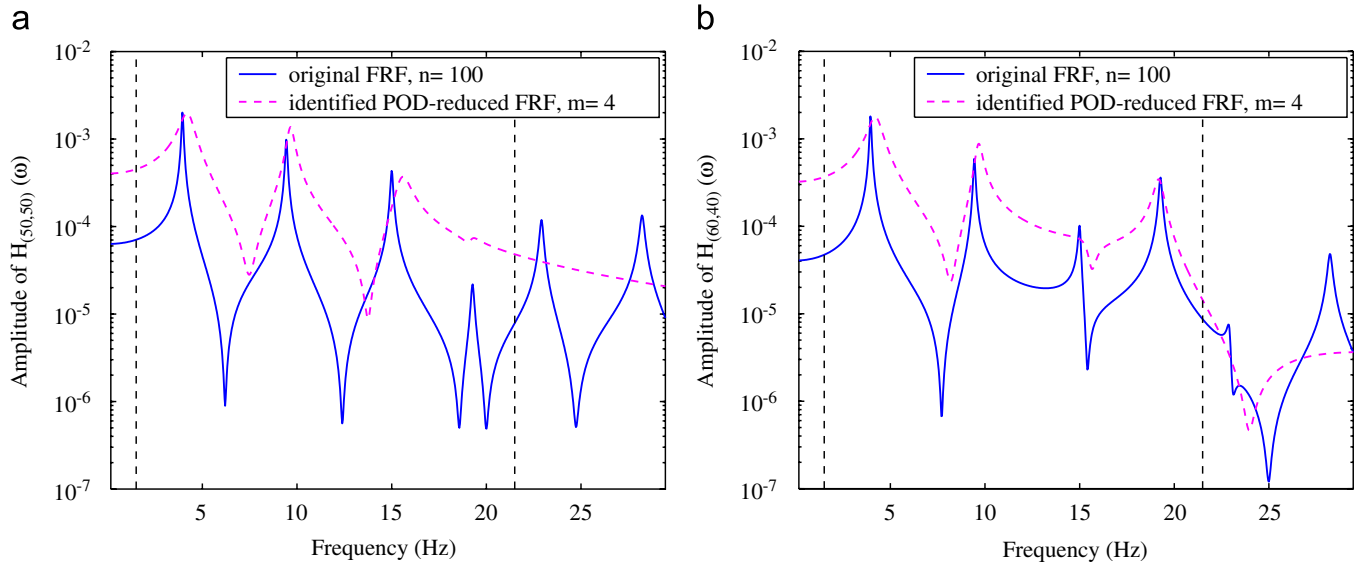

Fig. 17. Original and identified POD-reduced FRFs under an SNR of 10 dB for frequency band 2. (a) Driving-point-FRF and (b) cross-FRF.

priori through POD eigenvalue analysis as in the forward simulation problem (refer to Figs. 4–7). Next we estimate the reduced-order system matrices. These identified matrices are then used to construct typical FRFs of the system and compared to the FRFs of comprehensive models, as shown in Figs. 8–11. The symmetry constraint of the system matrices was applied in the identification process using Tikhonov regularisation, with the value for the regularisation parameters, λ_M, λ_C and λ_K all being 100 estimated through L-curve criterion. Note that the identified system matrices reproduce FRFs that match reasonably well the original FRFs.

6.2.2. *Reduced-order model identification: noisy case*

We have now demonstrated the efficacy of the proposed method for the case of noise-free data. In the low-frequency range, such assumption is perhaps reasonable as the signal-to-noise ratio (SNR) is sufficiently high for large-amplitude response. In the mid-frequency range, however, the SNR decreases significantly and

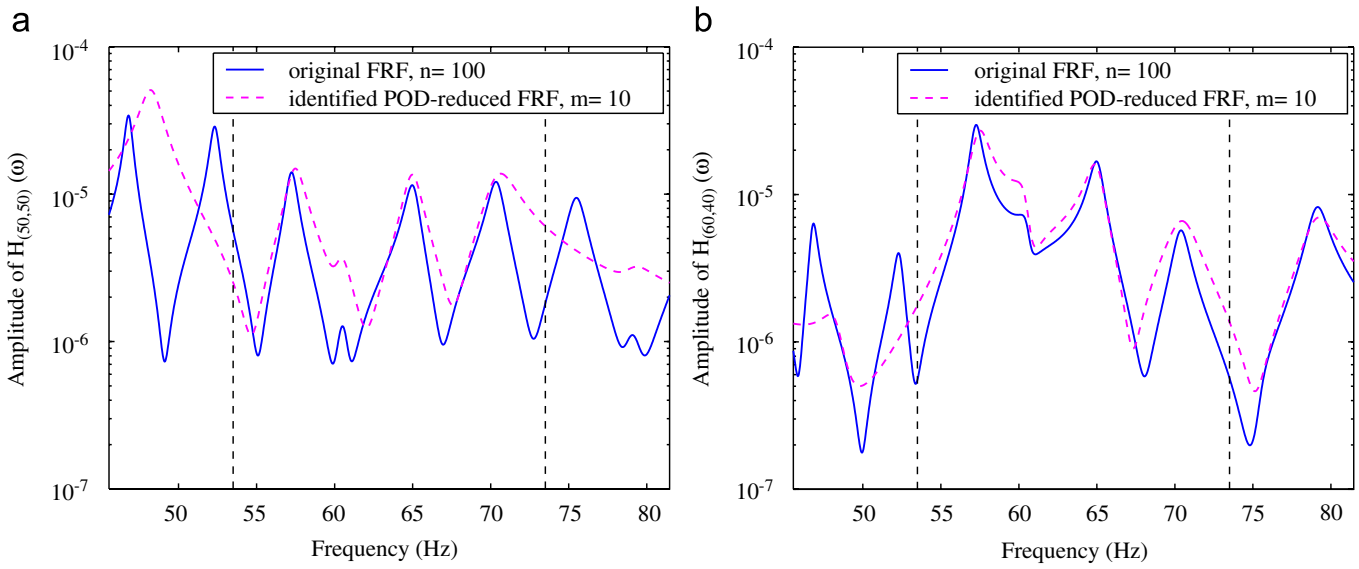

Fig. 18. Original and identified POD-reduced FRFs under an SNR of 10 dB for frequency band 3. (a) Driving-point-FRF and (b) cross-FRF.

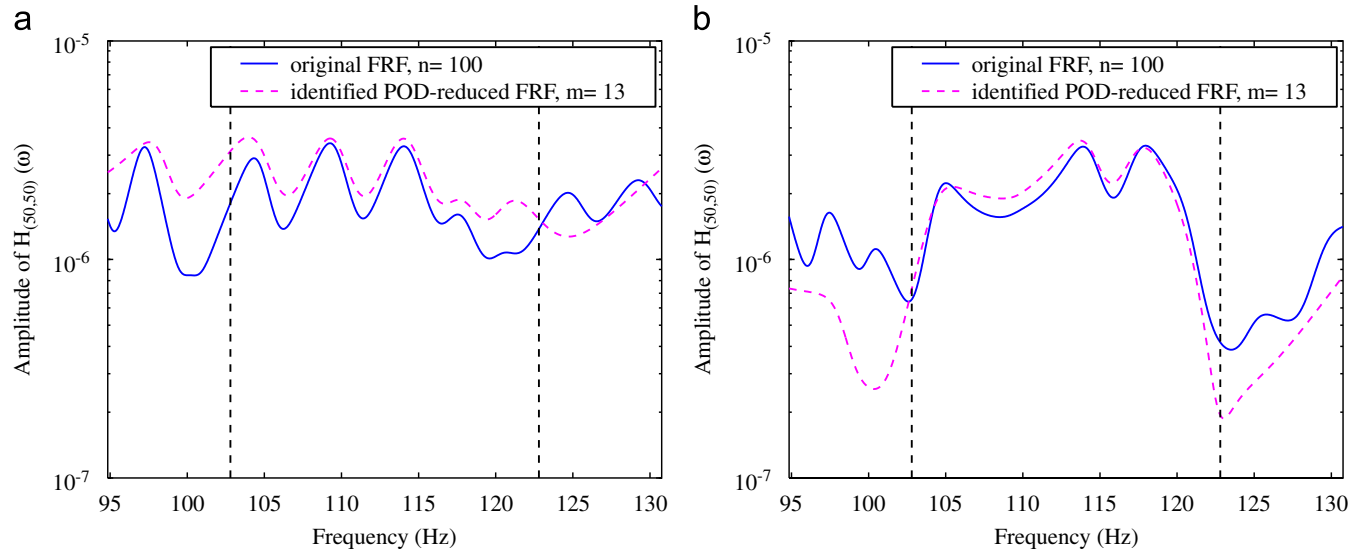

Fig. 19. Original and identified POD-reduced FRFs under an SNR of 10 dB for frequency band 4. (a) Driving-point-FRF and (b) cross-FRF.

thereby invalidates the noise-free assumption on the data arising from low-amplitude oscillations. In such cases, the presence of noise may significantly affect the confidence level of the estimated parameters.

Now we apply the same methodology described above with the additional effect of measurement noise on the system response, being modeled with uncorrelated Gaussian band-limited white noise. We consider the different cases of SNR prior to the identification process. Let σ_n^2 and σ_s^2 denote the variance of the noise and the original signal, respectively. The SNR is calculated using

$$\mathrm{SNR} = 10 \log_{10} \frac{\sigma_s^2}{\sigma_n^2} \,\mathrm{dB}. \tag{53}$$

Thus, an SNR of 10 implies that the variance of the signal is 10 times higher than the variance of the contaminating noise. An SNR of 20 indicates that the variance of the signal is 100 times higher than the variance of the contaminating noise. With an SNR of 20 dB, we obtain the identified FRF shown in Figs. 12–15. Compared to the noiseless case, a noise level resulting in an SNR of 20 dB does not seem to alter the identified system much. With an SNR of 10 dB (higher noise levels), we reproduce the FRFs using identified reduced model shown in Figs. 16–19. Compared to the identified FRF in the case of 20 dB of the SNR, a higher noise level of 10 dB SNR results in worse estimate of the FRF as expected. However, an SNR of 10 implies a noise amplitude that is on average $\sqrt{10} \approx 3.2$ times smaller than that of the original signal. In such case of a high noise level, the proposed identification method still performs reasonably well which is encouraging.

7. Conclusion

This paper explored the feasibility of identifying a reduced-order model of linear dynamical system in the mid-frequency regime. POD was used for the model reduction strategy. Such a reduced-order model circumvents the limitations of traditional modal analysis developed for the low-frequency region. The inverse problem relating to the identification of the mass, damping and stiffness matrices was tackled in the framework of a linear least-square estimation. Kronecker algebra was used to systematically handle the proposed mathematical operations. Tikhonov regularisation was applied to satisfy certain physical constraints defining the symmetry of the identified matrices involving linear self-adjoint operators. The salient features that emerged from the current investigation are:

(1) For the discrete dynamical system investigated in this paper, it is demonstrated that POD can be successfully applied for the reduced-order modelling. The dimension of the reduced model may be an order of magnitude smaller than the corresponding comprehensive model.
(2) A Kronecker algebraic framework permits a general and concise theoretical formulation for the identification of the system matrices in the linear least-square sense. Subsequently, the mathematical framework is generalised to incorporate Tikhonov regularisation to achieve the symmetry property of the mass, damping and stiffness matrices.
(3) The predictions from the identified reduced-order models match reasonably well with the original system response. The robustness of the identification method was demonstrated by a noise-sensitivity study.

This initial numerical study suggests that it might be possible to put the method into practice. However, much remains to be done to validate, test and extend both the theory and the methods for practical application. Future works would consider experimental testing of the proposed procedure and application to more complex real-life dynamical systems.

Acknowledgements

The first author acknowledges the support of the National Sciences and Engineering Research Council of Canada through the award of a Canada Graduate Scholarship. The second author acknowledges the support of the UK Engineering and Physical Sciences Research Council (EPSRC) through the award of an Advanced Research Fellowship and the Royal Society of London for the award of a visiting fellowship at Carleton

University, Canada. The third author acknowledges the support of a Discovery Grant from National Sciences and Engineering Research Council of Canada and the Canada Research Chair Program.

Appendix A. Background of Kronecker algebra

A.1. Kronecker product

Given a matrix $\mathbf{A}$ of order $m \times n$ and a matrix $\mathbf{B}$ of order $p \times q$ represented by

$$\mathbf{A} = \begin{bmatrix} a_{11} & \cdots & a_{1n} \\ \vdots & \ddots & \vdots \\ a_{m1} & \cdots & a_{mn} \end{bmatrix} \tag{A.1}$$

and

$$\mathbf{B} = \begin{bmatrix} b_{11} & \cdots & b_{1q} \\ \vdots & \ddots & \vdots \\ b_{p1} & \cdots & b_{pq} \end{bmatrix}, \tag{A.2}$$

the Kronecker product of $\mathbf{A}$ and $\mathbf{B}$ results in a matrix of order $mp \times nq$ given by [44]

$$\mathbf{A} \otimes \mathbf{B} = \begin{bmatrix} a_{11}\mathbf{B} & \cdots & a_{1n}\mathbf{B} \\ \vdots & \ddots & \vdots \\ a_{m1}\mathbf{B} & \cdots & a_{mn}\mathbf{B} \end{bmatrix}. \tag{A.3}$$

A.2. Vectorisation

Given a matrix $\mathbf{A}$ of order $m \times n$ represented by

$$\mathbf{A} = [\,\mathbf{A}_{\cdot 1} \quad \mathbf{A}_{\cdot 2} \quad \cdots \quad \mathbf{A}_{\cdot n}\,] \tag{A.4}$$

in which $\mathbf{A}_{\cdot i}$ denotes the ith column of $\mathbf{A}$, the vectorisation of $\mathbf{A}$ results in a column vector of order mn given by [44]

$$\mathrm{vec}(\mathbf{A}) = \begin{bmatrix} \mathbf{A}_{\cdot 1} \\ \mathbf{A}_{\cdot 2} \\ \vdots \\ \mathbf{A}_{\cdot n} \end{bmatrix}. \tag{A.5}$$

Appendix B. Mass matrix symmetry constraint

The mass matrix $\mathbf{M}_m$ can be rewritten as

$$\mathbf{M}_m = [\,\mathbf{I}_m \quad \mathbf{0}_{m\times m} \quad \mathbf{0}_{m\times m}\,] \begin{bmatrix} \mathbf{M}_m \\ \mathbf{C}_m \\ \mathbf{K}_m \end{bmatrix} = [\,\mathbf{I}_m \quad \mathbf{0}_{m\times m} \quad \mathbf{0}_{m\times m}\,] \begin{bmatrix} \mathbf{M}_m \\ \mathbf{C}_m \\ \mathbf{K}_m \end{bmatrix} \mathbf{I}_m, \tag{B.1}$$

where $\mathbf{0}_{m\times m}$ is the square matrix of order $m\times m$ whose elements are zero. Similarly, $\mathbf{M}_m^{\mathrm{T}}$ can be rewritten as

$$\mathbf{M}_m^{\mathrm{T}} = [\,\mathbf{M}_m^{\mathrm{T}} \quad \mathbf{C}_m^{\mathrm{T}} \quad \mathbf{K}_m^{\mathrm{T}}\,]\begin{bmatrix}\mathbf{I}_m\\ \mathbf{0}_{m\times m}\\ \mathbf{0}_{m\times m}\end{bmatrix}$$

$$= \begin{bmatrix}\mathbf{M}_m\\ \mathbf{C}_m\\ \mathbf{K}_m\end{bmatrix}^{\mathrm{T}}\begin{bmatrix}\mathbf{I}_m\\ \mathbf{0}_{m\times m}\\ \mathbf{0}_{m\times m}\end{bmatrix} = \mathbf{I}_m\begin{bmatrix}\mathbf{M}_m\\ \mathbf{C}_m\\ \mathbf{K}_m\end{bmatrix}^{\mathrm{T}}\begin{bmatrix}\mathbf{I}_m\\ \mathbf{0}_{m\times m}\\ \mathbf{0}_{m\times m}\end{bmatrix}. \tag{B.2}$$

The symmetry constraint (36) can be written as

$$\mathbf{M}_m = \mathbf{M}_m^{\mathrm{T}}. \tag{B.3}$$

Applying the vec operator (see Section A.2 of Appendix A) to both sides of (B.3) yields

$$\mathrm{vec}(\mathbf{M}_m) = \mathrm{vec}(\mathbf{M}_m^{\mathrm{T}}). \tag{B.4}$$

Substituting expressions (B.1) and (B.2) into (B.4), we obtain

$$\mathrm{vec}\left([\,\mathbf{I}_m \quad \mathbf{0}_{m\times m} \quad \mathbf{0}_{m\times m}\,]\begin{bmatrix}\mathbf{M}_m\\ \mathbf{C}_m\\ \mathbf{K}_m\end{bmatrix}\mathbf{I}_m\right) = \mathrm{vec}\left(\mathbf{I}_m\begin{bmatrix}\mathbf{M}_m\\ \mathbf{C}_m\\ \mathbf{K}_m\end{bmatrix}^{\mathrm{T}}\begin{bmatrix}\mathbf{I}_m\\ \mathbf{0}_{m\times m}\\ \mathbf{0}_{m\times m}\end{bmatrix}\right). \tag{B.5}$$

Applying the Kronecker algebra identity $\mathrm{vec}(\mathbf{AYB}) = (\mathbf{B}^{\mathrm{T}}\otimes\mathbf{A})\,\mathrm{vec}(\mathbf{Y})$ [44] to (B.5), we obtain

$$(\mathbf{I}_m\otimes[\,\mathbf{I}_m \quad \mathbf{0}_{m\times m} \quad \mathbf{0}_{m\times m}\,])\mathrm{vec}\left(\begin{bmatrix}\mathbf{M}_m\\ \mathbf{C}_m\\ \mathbf{K}_m\end{bmatrix}\right)$$

$$= ([\,\mathbf{I}_m \quad \mathbf{0}_{m\times m} \quad \mathbf{0}_{m\times m}\,]\otimes\mathbf{I}_m)\mathrm{vec}\left(\begin{bmatrix}\mathbf{M}_m\\ \mathbf{C}_m\\ \mathbf{K}_m\end{bmatrix}^{\mathrm{T}}\right). \tag{B.6}$$

The vec-permutation matrix $\mathbf{U}$ can be used to make the following relation [53]:

$$\mathrm{vec}\left(\begin{bmatrix}\mathbf{M}_m\\ \mathbf{C}_m\\ \mathbf{K}_m\end{bmatrix}^{\mathrm{T}}\right) = \mathbf{U}\,\mathrm{vec}\left(\begin{bmatrix}\mathbf{M}_m\\ \mathbf{C}_m\\ \mathbf{K}_m\end{bmatrix}\right). \tag{B.7}$$

Substituting (B.7) into (B.6), one obtains

$$(\mathbf{I}_m\otimes[\,\mathbf{I}_m \quad \mathbf{0}_{m\times m} \quad \mathbf{0}_{m\times m}\,])\mathrm{vec}\left(\begin{bmatrix}\mathbf{M}_m\\ \mathbf{C}_m\\ \mathbf{K}_m\end{bmatrix}\right)$$

$$= ([\,\mathbf{I}_m \quad \mathbf{0}_{m\times m} \quad \mathbf{0}_{m\times m}\,]\otimes\mathbf{I}_m)\mathbf{U}\,\mathrm{vec}\left(\begin{bmatrix}\mathbf{M}_m\\ \mathbf{C}_m\\ \mathbf{K}_m\end{bmatrix}\right) \tag{B.8}$$

which is equivalent to

$$\left\{\begin{array}{c}(\mathbf{I}_m \otimes [\,\mathbf{I}_m \quad \mathbf{0}_{m\times m} \quad \mathbf{0}_{m\times m}\,]) \\ -([\,\mathbf{I}_m \quad \mathbf{0}_{m\times m} \quad \mathbf{0}_{m\times m}\,] \otimes \mathbf{I}_m)\mathbf{U}\end{array}\right\} \mathrm{vec}\left(\begin{bmatrix}\mathbf{M}_m \\ \mathbf{C}_m \\ \mathbf{K}_m\end{bmatrix}\right) = 0_{m^2}. \tag{B.9}$$

The constraint (B.9) can be rewritten as

$$\mathbf{L}_M \mathbf{x} = 0_{m^2}, \tag{B.10}$$

where

$$\mathbf{L}_M = [(\mathbf{I}_m \otimes [\,\mathbf{I}_m \quad \mathbf{0}_{m\times m} \quad \mathbf{0}_{m\times m}\,]) - ([\,\mathbf{I}_m \quad \mathbf{0}_{m\times m} \quad \mathbf{0}_{m\times m}\,] \otimes \mathbf{I}_m)\mathbf{U}]. \tag{B.11}$$

References

[1] M. Géradin, D. Rixen, Mechanical Vibrations (Théorie des Vibrations, Trans.), second ed., Wiley, New York, NY, 1997.
[2] R.W. Clough, J. Penzien, Dynamics of Structures, McGraw-Hill, New York, 1975.
[3] J. Humar, Dynamics of Structures, Prentice-Hall, Englewood Cliffs, NJ, 1990.
[4] N.M.M. Maia, J.M.M. Silva, Theoretical and Experimental Modal Analysis, Research Studies Press, 1997.
[5] D.J. Ewins, Modal Testing: Theory and Practice, second ed., Research Studies Press, 2000.
[6] U. Iemma, L. Moreno, M. Diez, Digital holography and Karhunen–Loève decomposition for the modal analysis of two-dimensional vibrating structures, Journal of Sound and Vibration 291 (1–2) (2006) 107–131.
[7] P. Lancaster, Expression of damping matrices in linear vibration problems, Journal of Aerospace Sciences 28 (1961) 256.
[8] S.R. Ibrahim, Dynamic modelling of structures from measured complex modes, AIAA Journal 21 (6) (1983) 898–901.
[9] S. Adhikari, Lancaster's method of damping identification revisited, Journal of Vibration and Acoustics 124 (4) (2002) 617–627.
[10] M. Baruch, Correction of stiffness matrix using vibration tests, AIAA Journal 20 (3) (1982) 441–442.
[11] M. Baruch, Optimal correction of mass and stiffness matrices using measured modes, AIAA Journal 20 (11) (1982) 1623–1626.
[12] M. Baruch, Methods of reference basis for identification of linear dynamic structures, AIAA Journal 22 (4) (1984) 561–564.
[13] M.J. Roemer, D.J. Mook, Mass, stiffness and damping matrix identification: an integrated approach, Journal of Vibration and Acoustics 114 (1992) 358–363.
[14] S.Y. Chen, M.S. Ju, Y.G. Tsuei, Estimation of mass, stiffness and damping matrices from frequency response function, Journal of Vibration and Acoustics 118 (1996) 78–82.
[15] X. Zhao, Y.L. Xu, J. Li, J. Chen, Hybrid identification method for multi-story buildings with unknown ground motion: theory, Journal of Sound and Vibration 291 (1–2) (2006) 215–239.
[16] B.F. Yan, A. Miyamoto, E.G. Bruhwiler, Wavelet transform-based modal parameter identification considering uncertainty, Journal of Sound and Vibration 291 (1–2) (2006) 285–301.
[17] R. Provasi, G.A. Zanetta, The extended Kalman filter in the frequency domain for the identification of mechanical structures excited by sinusoidal multiple inputs, Mechanical Systems and Signal Processing 14 (3) (2000) 327–341.
[18] A. Srikantha-Phani, J. Woodhouse, The challenge of reliable identification of complex modes, in: Proceedings of the IMAC-XX, 20th International Modal Analysis Conference, Los Angeles, USA, 2002.
[19] S. Adhikari, Optimal complex modes and an index of damping non-proportionality, Mechanical System and Signal Processing 18 (1) (2004) 1–27.
[20] L. Brillouin, Wave Propagation in Periodic Structures: Electric Filters and Crystal Lattices, Dover, New York, 1953.
[21] A.D. Nashif, D.I.G. Jones, J.P. Henderson, Vibration Damping, Wiley, New York, 1985.
[22] C.T. Sun, Y.P. Lu, Vibration Damping of Structural Elements, Prentice-Hall PTR, NJ, USA, 1995.
[23] B.F. Smith, P.E. Bjrstad, W.D. Gropp, Domain Decomposition: Parallel Multilevel Methods for Elliptic Partial Differential Equations, Cambridge University Press, Cambridge, 1996.
[24] A. Quarteroni, A. Valli, Domain Decomposition Methods for Partial Differential Equations, Clarendon Press, Oxford, 1999.
[25] A. Toselli, O. Widlund, Domain Decomposition Methods—Algorithms and Theory, Springer, Berlin, 2005.
[26] H.A. van der Vorst, Iterative Krylov Methods for Large Linear Systems, Cambridge Monographs on Applied and Computational Mathematics, vol. 13, Cambridge University Press, Cambridge, 2003.
[27] Y. Saad, Iterative Methods for Sparse Linear Systems, second ed., SIAM, Philadelphia, PA, 2003.
[28] A. Sarkar, R. Ghanem, Mid-frequency structural dynamics with parameter uncertainty, Computer Methods in Applied Mechanics and Engineering 191 (47–48) (2002) 5499–5513.
[29] A. Sarkar, M.P. Paidoussis, A compact limit-cycle oscillation model of a cantilever conveying fluid, Journal of Fluids and Structures 17 (4) (2003) 525–539.

[30] A. Sarkar, M.P. Paidoussis, A cantilever conveying fluid: coherent modes versus beam modes, International Journal of Non-Linear Mechanics 39 (3) (2004) 467–481.
[31] G. Kerschen, J.C. Golinval, Physical interpretation of the proper orthogonal modes using the singular value decomposition, Journal of Sound and Vibration 249 (5) (2002) 849–865.
[32] M.F.A. Azeez, A.F. Vakakis, Numerical and experimental analysis of the nonlinear dynamics due to impacts of a continuous overhung rotor, in: Proceedings of DETC97, ASME Design Engineering Technical Conferences, Sacramento, USA, 1997.
[33] M.F.A. Azeez, A.F. Vakakis, Proper orthogonal decomposition of a class of vibroimpact oscillations, Journal of Sound and Vibration 240 (5) (2001) 859–889.
[34] G. Kerschen, J.C. Golinval, Non-linear generalization of principal component analysis: from a global to a local approach, Journal of Sound and Vibration 254 (5) (2002) 867–876.
[35] G. Kerschen, B.F. Feeny, J.C. Golinval, On the exploitation of chaos to build reduced-order models, Computer Methods in Applied Mechanics and Engineering 192 (2003) 1785–1795.
[36] G. Kerschen, J.C. Golinval, Generation of accurate finite element models of nonlinear systems application to an aeroplane-like structure, Nonlinear Dynamics 39 (2003) 129–142.
[37] K. Kunisch, S. Volkwein, Galerkin proper orthogonal decomposition methods for a general equation in fluid dynamics, SIAM Journal on Numerical Analysis 40 (2) (2002) 492–515.
[38] V. Lenaerts, G. Kerschen, J.C. Golinval, Proper orthogonal decomposition for model updating of non-linear mechanical systems, Mechanical Systems and Signal Processing 15 (1) (2001) 31–43.
[39] V. Lenaerts, G. Kerschen, J.-C. Golinval, Identification of a continuous structure with a geometrical non-linearity. Part ii: proper orthogonal decomposition, Journal of Sound and Vibration 262 (4) (2003) 907–919.
[40] B.F. Feeny, R. Kappagantu, On the physical interpretation of proper orthogonal modes in vibrations, Journal of Sound and Vibration 211 (4) (1998) 607–616.
[41] K. Worden, G.R. Tomlinson, Nonlinearity in Structural Dynamics: Detection, Identification and Modelling, Institute of Physics, London, 2000.
[42] A. Sarkar, R. Ghanem, A substructure approach for the midfrequency vibration of stochastic systems, Journal of the Acoustical Society of America 113 (4) (2003) 1922–1934.
[43] M. Khalil, Reduced order linear system identification, Master's Thesis, Carleton University, Ottawa, Canada, 2006.
[44] A. Graham, Kronecker Products and Matrix Calculus: With Applications, Ellis Horwood, Chichester, UK, 1981.
[45] M. Khalil, S. Adhikari, A. Sarkar, Identification of damping using proper orthogonal decomposition, in: B.H.V. Topping, G. Montero, R. Montenegro (Eds.), Proceedings of the Eighth International Conference on Computational Structures Technology, Stirlingshire, United Kingdom, Civil-Comp Press, paper 73, 2006.
[46] R. Penrose, A generalized inverse for matrices, Mathematical Proceedings of the Cambridge Philosophical Society 51 (1955) 406–413.
[47] H. Sorenson, Parameter Estimation—Principles and Problems, Marcel Dekker, New York, 1980.
[48] A.N. Tikhonov, V.Y. Arsenin, Solutions of Ill-Posed Problems, Winston-Wiley, 1977.
[49] R. Hunt, Three-dimensional flow in a general tube using a combination of finite and pseudospectral discretisations, SIAM Journal on Scientific Computing 16 (3) (1995) 513–530.
[50] M. Hanke, P.C. Hansen, Regularization methods for large-scale problems, Surveys on Mathematics for Industry 3 (1993) 253–315.
[51] P.C. Hansen, Numerical tools for analysis and solution of Fredholm integral equations of the first kind, Inverse Problems 8 (6) (1992) 849–872.
[52] P.C. Hansen, A matlab package for analysis and solution of discrete ill-posed problems, Numerical Algorithms 6 (1994) 1–35.
[53] H.V. Henderson, S.R. Searle, The vec-permutation matrix, the vec operator and Kronecker products: a review, Linear and Multilinear Algebra 9 (1981) 271–288.